



TECH BRIEFS

NATIONAL AERONAUTICS AND SPACE ADMINISTRATION

-  Technology Focus
-  Electronics/Computers
-  Software
-  Materials
-  Mechanics/Machinery
-  Manufacturing
-  Bio-Medical
-  Physical Sciences
-  Information Sciences
-  Books and Reports

INTRODUCTION

Tech Briefs are short announcements of innovations originating from research and development activities of the National Aeronautics and Space Administration. They emphasize information considered likely to be transferable across industrial, regional, or disciplinary lines and are issued to encourage commercial application.

Availability of NASA Tech Briefs and TSPs

Requests for individual Tech Briefs or for Technical Support Packages (TSPs) announced herein should be addressed to

National Technology Transfer Center

Telephone No. **(800) 678-6882** or via World Wide Web at **www.nttc.edu**

Please reference the control numbers appearing at the end of each Tech Brief. Information on NASA's Innovative Partnerships Program (IPP), its documents, and services is also available at the same facility or on the World Wide Web at **<http://www.nasa.gov/offices/ipp/network/index.html>**

Innovative Partnerships Offices are located at NASA field centers to provide technology-transfer access to industrial users. Inquiries can be made by contacting NASA field centers listed below.

NASA Field Centers and Program Offices

Ames Research Center
Lisa L. Lockyer
(650) 604-1754
lisa.l.lockyer@nasa.gov

Dryden Flight Research Center
Yvonne D. Gibbs
(661) 276-3720
yvonne.d.gibbs@nasa.gov

Glenn Research Center
Kathy Needham
(216) 433-2802
kathleen.k.needham@nasa.gov

Goddard Space Flight Center
Nona Cheeks
(301) 286-5810
nona.k.cheeks@nasa.gov

Jet Propulsion Laboratory
Andrew Gray
(818) 354-4906
gray@jpl.nasa.gov

Johnson Space Center
information
(281) 483-3809
jsc.techtran@mail.nasa.gov

Kennedy Space Center
David R. Makufka
(321) 867-6227
david.r.makufka@nasa.gov

Langley Research Center
Elizabeth B. Plentovich
(757) 864-2857
elizabeth.b.plentovich@nasa.gov

Marshall Space Flight Center
Jim Dowdy
(256) 544-7604
jim.dowdy@msfc.nasa.gov

Stennis Space Center
Ramona Travis
(228) 688-3832
ramona.e.travis@nasa.gov

Carl Ray, Program Executive
Small Business Innovation
Research (SBIR) & Small
Business Technology
Transfer (STTR) Programs
(202) 358-4652
carl.g.ray@nasa.gov

Doug Comstock, Director
Innovative Partnerships
Program Office
(202) 358-2221
doug.comstock@nasa.gov



TECH BRIEFS

NATIONAL AERONAUTICS AND SPACE ADMINISTRATION



5 Technology Focus: Test & Measurement

- 5 Instrument for Measuring Thermal Conductivity of Materials at Low Temperatures
- 5 Multi-Axis Accelerometer Calibration System
- 6 Pupil Alignment Measuring Technique and Alignment Reference for Instruments or Optical Systems
- 6 Autonomous System for Monitoring the Integrity of Composite Fan Housings
- 7 A Safe, Self-Calibrating, Wireless System for Measuring Volume of Any Fuel at Non-Horizontal Orientation



9 Electronics/Computers

- 9 Adaptation of the Camera Link Interface for Flight-Instrument Applications
- 9 High-Performance CCSDS Encapsulation Service Implementation in FPGA
- 10 High-Performance CCSDS AOS Protocol Implementation in FPGA
- 10 Advanced Flip Chips in Extreme Temperature Environments



11 Green Design

- 11 Diffuse-Illumination Systems for Growing Plants
- 12 Microwave Plasma Hydrogen Recovery System



13 Manufacturing & Prototyping

- 13 Producing Hydrogen by Plasma Pyrolysis of Methane
- 14 Self-Deployable Membrane Structures
- 14 Reactivation of a Tin-Oxide-Containing Catalyst



17 Materials

- 17 Functionalization of Single-Wall Carbon Nanotubes by Photo-Oxidation



19 Mechanics/Machinery

- 19 Miniature Piezoelectric Macro-Mass Balance
- 19 Acoustic Liner for Turbomachinery Applications
- 20 Metering Gas Strut for Separating Rocket Stages
- 20 Large-Flow-Area Flow-Selective Liquid/Gas Separator
- 21 Counterflowing Jet Subsystem Design
- 21 Water Tank With Capillary Air/Liquid Separation



23 Physical Sciences

- 23 True Shear Parallel Plate Viscometer
- 23 Focusing Diffraction Grating Element With Aberration Control
- 24 Universal Millimeter-Wave Radar Front End
- 24 Mode Selection for a Single-Frequency Fiber Laser
- 24 Qualification and Selection of Flight Diode Lasers for Space Applications
- 25 Plenoptic Imager for Automated Surface Navigation
- 25 Maglev Facility for Simulating Variable Gravity
- 26 Hybrid AlGaIn-SiC Avalanche Photodiode for Deep-UV Photon Detection
- 26 High-Speed Operation of Interband Cascade Lasers



27 Information Sciences

- 27 3D GeoWall Analysis System for Shuttle External Tank Foreign Object Debris Events
- 27 Charge-Spot Model for Electrostatic Forces in Simulation of Fine Particulates
- 28 Hidden Statistics Approach to Quantum Simulations
- 28 Reconstituted Three-Dimensional Interactive Imaging
- 29 Determining Atmospheric-Density Profile of Titan



31 Bio-Medical

- 31 Digital Microfluidics Sample Analyzer
- 31 Radiation Protection Using Carbon Nanotube Derivatives
- 32 Process to Selectively Distinguish Viable From Non-Viable Bacterial Cells



33 Software

- 33 TEAMS Model Analyzer
- 33 Probabilistic Design and Analysis Framework
- 33 Excavator Design Validation
- 34 Observing System Simulation Experiment (OSSE) for the HypIRI Spectrometer Mission
- 34 Momentum Management Tool for Low-Thrust Missions
- 35 Mixed Real/Virtual Operator Interface for ATHLETE
- 35 Antenna Controller Replacement Software
- 36 Efficient Parallel Engineering Computing on Linux Workstations
- 36 FAILSAFE Health Management for Embedded Systems
- 37 Water Detection Based on Sky Reflections
- 38 Nonlinear Combustion Instability Prediction
- 38 JMISR Interactive eXplorer

38	Characterization of Cloud Water-Content Distribution	44	Real-Time Exponential Curve Fits Using Discrete Calculus
39	Autonomous Planning and Replanning for Mine-Sweeping Unmanned Underwater Vehicles	45	Short-Block Protograph-Based LDPC Codes
39	Dayside Ionospheric Superfountain	46	Space Images for NASA/JPL
39	<i>In-Situ</i> Pointing Correction and Rover Microlocalization	47	Situational Lightning Climatologies
40	Operation Program for the Spatially Phase-Shifted Digital Speckle Pattern Interferometer — SPS-DSPI	48	Autonomous Exploration for Gathering Increased Science
40	GOATS - Orbitology Component	48	World Wide Web Metaphors for Search Mission Data
41	Hybrid-PIC Computer Simulation of the Plasma and Erosion Processes in Hall Thrusters	49	Optimal Codes for the Burst Erasure Channel
41	BioNet Digital Communications Framework	49	Phenological Parameters Estimation Tool
41	Real-Time Feature Tracking Using Homography	50	XMbodyinfo
42	Sparse Superpixel Unmixing for Hyperspectral Image Analysis	51	Centralized Alert-Processing and Asset Planning for Sensorwebs
42	Intelligent Patching of Conceptual Geometry for CFD Analysis	51	Support for Systematic Code Reviews With the SCRUB Tool
43	Stereo Imaging Tactical Helper	52	Numerical Mean Element Orbital Analysis With Morbiter
43	Planning and Execution for an Autonomous Aerobot	53	Systems Maintenance Automated Repair Tasks (SMART)
		53	NAIF Toolkit — Extended



Instrument for Measuring Thermal Conductivity of Materials at Low Temperatures

Applications include development of novel materials as well as quality control for materials and process requirements.

John F. Kennedy Space Center, Florida

With the advance of polymer and other non-metallic material sciences, whole new series of polymeric materials and composites are being created. These materials are being optimized for many different applications including cryogenic and low-temperature industrial processes. Engineers need these data to perform detailed system designs and enable new design possibilities for improved control, reliability, and efficiency in specific applications. One main area of interest is cryogenic structural elements and fluid handling components and other parts, films, and coatings for low-temperature application. An important thermal property of these new materials is the apparent thermal conductivity (k -value).

Thermal conductivity testing is needed as part of the physical characterization of these various new and innovative polymers and composites. The Cryogenics Test Laboratory (CTL) at Kennedy Space Center designed and built a cryostat test instrument to measure the thermal conductivity of these types of materials at low temperatures. The instrument, known as the Cup Cryostat, is a small-scale cryogenic boil-off calorimeter designed to de-

termine the apparent thermal conductivity (k -value in milliwatt per meter-Kelvin) of materials for cryogenic temperatures and specifically at large temperature differences. Boundary temperatures are typically 300 K and 80 K, or any temperature difference in this range. The instrument's direct measure of the rate of thermal-energy transfer (power, in watts) provides relative thermal performance among materials (i.e., comparative k -value).

The Cup Cryostat method provides thermal conductivity data under representative-usage conditions, including a large temperature difference (ΔT) that is typical for most cryogenic applications. The materials are tested in a way that approximates the way such material would be implemented to solve engineering design problems. The new method is therefore complementary to the small temperature difference data generated by existing standard methods. The Cup Cryostat uses moderate size 75-mm-diameter round specimens, which is reasonable for the production of novel research materials. Thicknesses of up to 13 mm are permitted, but a 6.5-mm thick specimen is typical. The Cup Cryostat also provides mechanical compression loading capability so that thermal

performance data can be obtained under representative mechanical loading. In addition to nitrogen, the Cup Cryostat can be operated with other fluids, such as Freon and other suitable liquid refrigerants. For porous materials, residual gases such as helium, air, nitrogen, argon, or carbon dioxide may be selected for the environmental condition. All tests are performed at ambient (room) pressure. The compact design of the Cup Cryostat allows for specimen installation, system preparation, and cryogenic testing to be completed in less than one day, which means that costly set-up within a vacuum chamber is avoided.

The Cup Cryostat is designed to determine the apparent thermal conductivity under representative-use conditions of large ΔT and also with appropriate compressive loading, as desired. The test is comparative in nature, so absolute values must be obtained by direct comparison with known materials.

This work was done by James Fesmire, Jared Sass, and Wesley Johnson of Kennedy Space Center. For more information, contact the Kennedy Space Center Innovative Partnerships Program Office at (321) 867-5033. KSC-13217

Multi-Axis Accelerometer Calibration System

Langley Research Center, Hampton, Virginia

A low-cost, portable, and simplified system has been developed that is suitable for *in-situ* calibration and/or evaluation of multi-axis inertial measurement instruments (e.g.,). This system overcomes facility restrictions and maintains or improves the calibration quality for users of accelerometer-based instruments with applications in avionics, experimental wind tunnel research, and force balance calibration applications. The apparatus quickly

and easily positions a multi-axis accelerometer system into a precisely known orientation suitable for *in-situ* quality checks and calibration. In addition, the system incorporates powerful and sophisticated statistical methods, known as response surface methodology and statistical quality control. These methods improve calibration quality, reduce calibration time, and allow for increased calibration frequency, which enables the monitoring

of instrument stability over time. This technology overcomes the limitations and restrictions on accelerometer calibration facilities by:

- Minimizing reliance on a fixed calibration system,
- Leveraging the user's data acquisition system,
- Allowing for increased calibration frequency due to improved accessibility, and
- Automatically compensating for local gravitational field.

The cuboidal positioning system can be used to calibrate or evaluate single, dual, or triaxial packages. The system employs a simplified, linear mathematical model that is a function of gravitational components.

At the time of this reporting, NASA has built six systems in support of program operations. Further development is expected to expand the system's capabilities to other instruments and to complete temperature characterization.

This work was done by Tom Finley and Peter Parker of Langley Research Center. For further information, contact the Langley Innovative Partnerships Office at (757) 864-8881. LAR-17163-1

Pupil Alignment Measuring Technique and Alignment Reference for Instruments or Optical Systems

This technique can be used in any instrumentation that requires measurement of pupil alignment, such as optical instruments and cameras.

Goddard Space Flight Center, Greenbelt, Maryland

A technique was created to measure the pupil alignment of instruments *in situ* by measuring calibrated pupil alignment references (PARs) in instruments. The PAR can also be measured using an alignment telescope or an imaging system. PAR allows the verification of the science instrument (SI) pupil alignment at the integrated science instrument module (ISIM) level of assembly at ambient and cryogenic operating temperature. This will allow verification of the ISIM+SI alignment, and provide feedback to realign the SI if necessary.

This innovation consists of a 10-mm reflective patch on the +V1 face of a filter or closed position of the SI pupil wheel. The PAR will have a centered alignment crosshair and a minimum of two concentric circular fiducials representing a reference for the SI pupil alignment. The fiducials need not be exactly centered to the nominal SI pupil position, but their alignment relative to the nominal pupil position must be known to 0.2-percent of the pupil diameter. A clocking reference point should also be included in one quadrant to provide a reference.

The SI teams will reference their pupil alignment to the PAR during their instrument alignment, and measure the PAR in the +V1 horizontal and +V1 down ori-

entation at ambient temperature relative to the nominal V Coordinate system. The teams must demonstrate by test and analysis that the SI internal pupil alignment (from the kinematic feet up) is within the 0.5-percent placement allocation in 0-G. In addition, the SI team must demonstrate by test and analysis that the pupil alignment is within the 1-percent placement allocation in 1-G to a knowledge tolerance of 0.5 percent.

For ISIM, the PAR will be used at ambient temperature to verify that the SI has been installed to within allocated tolerances, and that its alignment does not shift due to vibration and other environmental test exposures. Ambient temperature measurements are performed using a PAR ISIM reference fixture to place alignment telescopes along the nominal chief center ray of each SI. The alignment telescopes will measure the offset of each SI PAR from nominal, and verify that the ISIM+SI alignment is within tolerance at ambient temperature. This also allows a non-invasive means of checking SI alignment to ISIM (without removing the ISIM enclosure) after shipping to observatory testing.

During the ISIM level verification, the OSIM will be aligned to ISIM and the optical telescope element (OTE) SIMu-

lator (OSIM) pupil reference fiducials will be projected onto the SI PARs, and the pupil alignment will be mapped. A Global Nominal Pupil (GNP) position, optimizing all of the SIs, will be determined, and used to align the ISIM to the OTE to minimize common path pupil alignment error. The pupil alignment measurement will also verify that the ISIM+SI pupil alignment is within allocated tolerances for all SIs in the +V1 down orientation. Therefore, it is crucial that the SI pupil alignments are known in both orientations for each SI. The final opportunity to discover and correct ISIM+SI pupil alignment errors at cryogenic operating temperature is during ISIM level testing, so it is crucial that a standardized reference (SI PAR) be available. These references will be measured relative to Pupil Imaging Modes for NIRCcam and MIRI to verify that the alignment has not changed downstream of the Pupil reference due to shifts of optics, and is the only way to deterministically demonstrate an unvignetted field at the observatory level of assembly.

This work was done by John G. Hagopian of Goddard Space Flight Center. For further information, contact the Goddard Innovative Partnerships Office at (301) 286-5810. GSC-15783-1

Autonomous System for Monitoring the Integrity of Composite Fan Housings

John H. Glenn Research Center, Cleveland, Ohio

A low-cost and reliable system assesses the integrity of composite fan-containment structures. The system utilizes a network of miniature sensors integrated with the structure to scan the entire

structural area for any impact events and resulting structural damage, and to monitor degradation due to usage. This system can be used to monitor all types of composite structures on aircraft and

spacecraft, as well as automatically monitor in real time the location and extent of damage in the containment structures. This diagnostic information is passed to prognostic modeling that is

being developed to utilize the information and provide input on the residual strength of the structure, and maintain a history of structural degradation during usage. The structural health-monitoring system would consist of three major components: (1) sensors and a sensor network, which is permanently bonded

onto the structure being monitored; (2) integrated hardware; and (3) software to monitor *in-situ* the health condition of in-service structures.

This work was done by Xinlin P. Qing, Christopher Aquino, and Amrita Kumar of Acellent Technologies, Inc. for Glenn Research Center.

Inquiries concerning rights for the commercial use of this invention should be addressed to NASA Glenn Research Center, Innovative Partnerships Office, Attn: Steve Fedor, Mail Stop 4-8, 21000 Brookpark Road, Cleveland, Ohio 44135. Refer to LEW-18396-1.

A Safe, Self-Calibrating, Wireless System for Measuring Volume of Any Fuel at Non-Horizontal Orientation

This system can be used for any fluid, including cryogenic and caustic liquids.

Langley Research Center, Hampton, Virginia

A system for wirelessly measuring the volume of fluid in tanks at non-horizontal orientation is predicated upon two technologies developed at Langley Research Center. The first is a magnetic field response recorder that powers and interrogates magnetic field response sensors [“Magnetic Field Response Measurement Acquisition System,” (LAR-16908), *NASA Tech Briefs*, Vol. 30, No. 6 (June 2006), page 28]. Magnetic field response sensors are a class of sensors that are powered via oscillating magnetic fields and when electrically active respond with their own magnetic fields whose attributes are dependent upon the magnitude of the physical quantity being measured. The response recorder facilitates the use of the second technology, which is a magnetic field re-

sponse fluid-level sensor [“Wireless Fluid-Level Sensors for Harsh Environments,” (LAR-17155), *NASA Tech Briefs*, Vol. 33, No. 4 (April 2009), page 30].

The method for powering and interrogating the sensors allows them to be completely encased in materials (Fig. 1) that are chemically resilient to the fluid being measured, thereby facilitating measurement of substances (e.g., acids, petroleum, cryogenic, caustic, and the like) that would normally destroy electronic circuitry. When the sensors are encapsulated, no fluid (or fluid vapor) is exposed to any electrical component of the measurement system. There is no direct electrical line from the vehicle or plant power into a fuel container. The means of interrogating and powering

the sensors can be completely physically and electrically isolated from the fuel and vapors by placing the sensor on the other side of an electrically non-conductive bulkhead (Fig. 2). These features prevent the interrogation system and its electrical components from becoming an ignition source.

Measuring fuel volume while the tank is not level would benefit aircraft during uncoordinated roll and pitch maneuvers, boat fuel tanks in heavy waves, and trucks, trains, and automobiles moving on steep inclines. The system can be used for any fluid, including cryogenic and caustic liquids. If the geometry of the tank is known, the surface defining the liquid/air interface can be determined by measuring the frequency re-

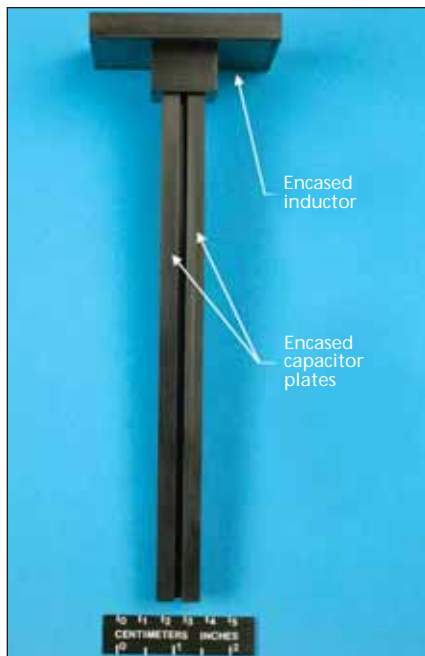


Figure 1. Magnetic Field Response Fluid-Level Sensor completely encapsulated in Ertalyte PET-P plastic.

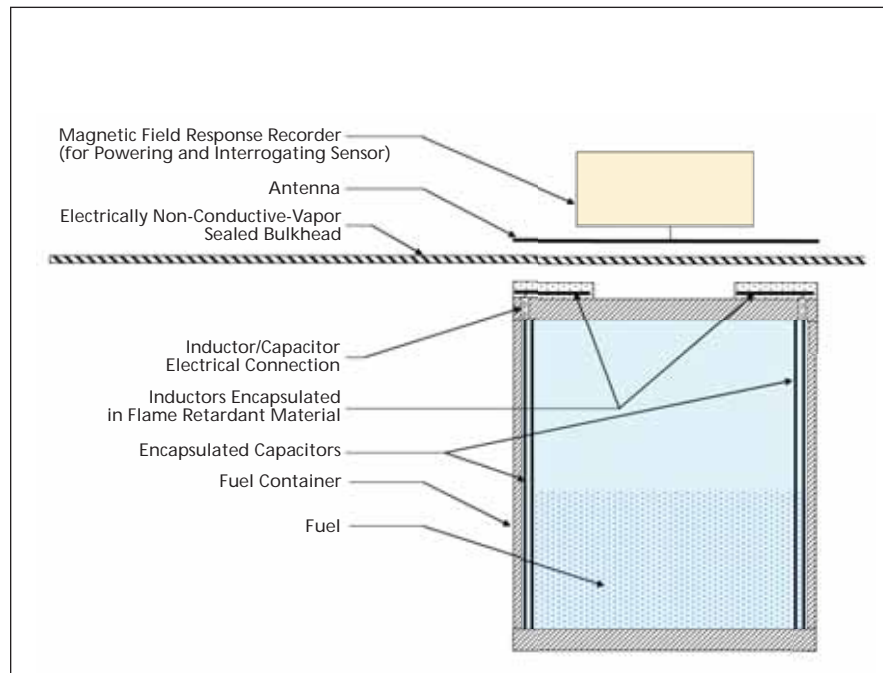


Figure 2. Fuel Tank With Encapsulated Sensors outboard bulkhead. Magnetic field response recorder and antenna are on other side of bulkhead.

sponse from at least three sensors in contact with the liquid. When internal baffles are used, the surface is that of a plane with fluid perturbations about the plane. When successive fuel-level readings are acquired and averaged, the results will approximate that of a plane. Once this surface is known, it can be used with the tank geometry to determine the volume under the surface.

Solely capacitive sensors are directly connected to power source and interrogation equipment. They must be calibrated for all capacitance in the sensor and the electrical wires to the sensor,

making it necessary to have the sensor electronics near or at the probe because lead length affects the capacitance of the probe. The magnetic field response sensor system presented provides an added logistical advantage in that electrical leads do not affect their calibration. Each sensor can easily be calibrated by taking the response frequency when the tank is empty, then again when the tank is full. One can then easily determine the sensor response with respect to the fractional fluid level without the need for additional measurements, and therefore know the frac-

tional level (e.g., 0.1 full) without knowing the fluid dielectric, sensor material, sensor geometry, or tank geometry. With the advent of vehicle engines using many different types of fuels with each having a different dielectric, it is advantageous for a measurement system that can easily be calibrated for any fluid without having to take the vehicle to a maintenance facility.

This work was done by Stanley E. Woodard of Langley Research Center and Bryant D. Taylor of ATK Space Division. Further information is contained in a TSP (see page 1). LAR-17116-1



Adaptation of the Camera Link Interface for Flight-Instrument Applications

NASA's Jet Propulsion Laboratory, Pasadena, California

COTS (commercial-off-the-shelf) hardware using an industry-standard Camera Link interface is proposed to accomplish the task of designing, building, assembling, and testing electronics for an airborne spectrometer that would be low-cost, but sustain the required data speed and volume. The focal plane electronics were designed to support that hardware standard. Analysis was done to determine how these COTS electronics could be interfaced with space-qualified camera electronics. Interfaces available for spaceflight application do not support the industry standard Camera Link interface, but with

careful design, COTS EGSE (electronics ground support equipment), including camera interfaces and camera simulators, can still be used.

The Camera Link data path is expandable. By adding another pair of interface circuits, and five more LVDS (low-voltage differential signaling) pairs (the "medium" Camera Link interface), the data rate can be doubled (4,080 Mbps). By adding a third pair of interface circuits and five more LVDS pairs (the "full" Camera Link interface), data rates of $64 \text{ bits} \times 85 \text{ MHz} = 5,440 \text{ Mbps}$ (over 5 Gbps) can be realized. The 28-bit commercial Camera Link interface is back-

wards compatible with the 21-bit space-qualified Channel Link interface. With proper circuit design and EGSE programming, the space-qualified chip set can be used to implement a compatible Camera Link interface using COTS Camera Link EGSE. COTS EGSE in the form of instrument (camera) simulators is also readily available. This allows easy, early checkout of the EGSE and flight systems.

This work was done by David P. Randall and John C. Mahoney of Caltech for NASA's Jet Propulsion Laboratory. For more information, contact iaoffice@jpl.nasa.gov. NPO-46991

High-Performance CCSDS Encapsulation Service Implementation in FPGA

This implementation can be used by telemetry receivers to process telemetry at high rates.

NASA's Jet Propulsion Laboratory, Pasadena, California

The Consultative Committee for Space Data Systems (CCSDS) Encapsulation Service is a convergence layer between lower-layer space data link framing protocols, such as CCSDS Advanced Orbiting System (AOS), and higher-layer networking protocols, such as CFDP (CCSDS File Delivery Protocol) and Internet Protocol Extension (IPE). CCSDS Encapsulation Service is considered part of the data link layer. The CCSDS AOS implementation is described in the preceding article. Recent advancement in RF modem technology has allowed multi-megabit transmission over space links. With this increase in data rate, the CCSDS Encapsulation Service needs to be optimized to both reduce energy consumption and operate at a high rate.

CCSDS Encapsulation Service has been implemented as an intellectual property core so that the aforementioned problems are solved by way of operating the CCSDS Encapsulation Service inside an FPGA. The CCSDS

Encapsulation Service in FPGA implementation consists of both packetizing and de-packetizing features.

Packetizer features include:

- Interfaces to fixed-sized framing layers such as CCSDS AOS or variable-sized framing layers such as CCSDS Telemetry command on the egress side.
- Interfaces to any octet-aligned data source that can provide start and end data delimiter signals on the ingress side.
- Idle insertion using 1-byte encapsulation packets.
- Interoperability tested with commercial off-the-shelf telemetry receiver implementation from RT-Logic.
- Includes statistical counters at packet, frame, and byte levels to facilitate data product accounting.

De-Packetizer features include:

- Interfaces to fixed-frame-size framing layers such as CCSDS AOS and telemetry on the ingress side.

- Filters out all types of idle CCSDS encapsulation packets.
- Includes a staging buffer to re-assemble all fragments of the higher-layer protocol packets before releasing to the egress side.
- Includes the ability to discard incomplete packets that are spanned over multiple frames.
- Includes statistical counters at packet, frame, and byte levels to facilitate data product accounting.

The combination of energy and performance optimization that embodies this design makes the work novel.

This work was done by Loren P. Clare, Jordan L. Torgerson, and Jackson Pang of Caltech for NASA's Jet Propulsion Laboratory. For more information, contact iaoffice@jpl.nasa.gov.

The software used in this innovation is available for commercial licensing. Please contact Daniel Broderick of the California Institute of Technology at danielb@caltech.edu. NPO-47167

High-Performance CCSDS AOS Protocol Implementation in FPGA

Telemetry receivers can use this implementation to process telemetry at high rates.

NASA's Jet Propulsion Laboratory, Pasadena, California

The Consultative Committee for Space Data Systems (CCSDS) Advanced Orbiting Systems (AOS) space data link protocol provides a framing layer between channel coding such as LDPC (low-density parity-check) and higher-layer link multiplexing protocols such as CCSDS Encapsulation Service, which is described in the following article. Recent advancement in RF modem technology has allowed multi-megabit transmission over space links. With this increase in data rate, the CCSDS AOS protocol implementation needs to be optimized to both reduce energy consumption and operate at a high rate.

CCSDS AOS has been implemented as an intellectual property core so that the aforementioned problems are solved by way of operating the CCSDS AOS inside a field-programmable gate array (FPGA).

The CCSDS AOS in FPGA implementation consists of both framing and de-framing features.

Features of the AOS Framer include:

- Fully customizable with respect to insert zone, virtual channel ID, and trailer fields.
- 8-bit parallel CCITT CRC16 calculation.
- First header pointer field calculation based on the data provided from the packet layers such as CCSDS Encapsulation Service or CCSDS Space Packet.
- Optimized for the Packet Service primitives with M_PDU.
- Available in byte-based or packet-based egress interface options.
- Statistical counters at both byte and frame levels to facilitate data product accountability.

Features of the AOS De-Framer include:

- Ingress buffer implementation to provide ingress processing overflow.

- 8-bit parallel CCITT CRC16 calculation and frame discard if CRC16 fails.
- First header pointer field extraction and forwarding to the de-packetizing layers such as CCSDS Encapsulation Service or CCSDS Packet Service.
- Optimized for the Packet Service primitives with M_PDU.
- Statistical counters at both byte and frame levels to facilitate data product accountability.

The combination of energy and performance optimization that embodies this design makes the work novel.

This work was done by Loren P. Clare, Jordan L. Torgerson, and Jackson Pang of Caltech for NASA's Jet Propulsion Laboratory. For more information, contact iaoffice@jpl.nasa.gov.

The software used in this innovation is available for commercial licensing. Please contact Daniel Broderick of the California Institute of Technology at danielb@caltech.edu. Refer to NPO-47166.

Advanced Flip Chips in Extreme Temperature Environments

This technology has application in avionics and electronics packaging.

NASA's Jet Propulsion Laboratory, Pasadena, California

The use of underfill materials is necessary with flip-chip interconnect technology to redistribute stresses due to mismatching coefficients of thermal expansion (CTEs) between dissimilar materials in the overall assembly. Underfills are formulated using organic polymers and possibly inorganic filler materials. There are a few ways to apply the underfills with flip-chip technology. Traditional capillary-flow underfill materials now possess high flow speed and reduced time to cure, but they still require additional processing steps beyond the typical surface-mount technology (SMT) assembly process.

Studies were conducted using underfills in a temperature range of -190 to 85 °C, which resulted in an increase of reliability by one to two orders of magnitude. Thermal shock of the flip-chip test articles was designed to induce failures at the interconnect sites (-40 to 100 °C). The study on the reliability of flip chips using underfills in the extreme tempera-

ture region is of significant value for space applications. This technology is considered as an enabling technology for future space missions.

Flip-chip interconnect technology is an advanced electrical interconnection approach where the silicon die or chip is electrically connected, face down, to the substrate by reflowing solder bumps on area-array metallized terminals on the die to matching footprints of solder-wettable pads on the chosen substrate. This advanced flip-chip interconnect technology will significantly improve the performance of high-speed systems, productivity enhancement over manual wire bonding, self-alignment during die joining, low lead inductances, and reduced need for attachment of precious metals.

The use of commercially developed no-flow fluxing underfills provides a means of reducing the processing steps employed in the traditional capillary flow methods to enhance SMT compati-

bility. Reliability of flip chips may be significantly increased by matching/tailoring the CTEs of the substrate material and the silicon die or chip, and also the underfill materials.

Advanced packaging interconnects technology such as flip-chip interconnect test boards have been subjected to various extreme temperature ranges that cover military specifications and extreme Mars and asteroid environments.

The eventual goal of each process step and the entire process is to produce components with 100 percent interconnect and satisfy the reliability requirements. Underfill materials, in general, may possibly meet demanding end use requirements such as low warpage, low stress, fine pitch, high reliability, and high adhesion.

This work was done by Rajeshuni Ramesh of Caltech for NASA's Jet Propulsion Laboratory. Further information is contained in a TSP (see page 1). NPO-41181



Diffuse-Illumination Systems for Growing Plants

Discrete sources produce spatially and spectrally mixed light.

Stennis Space Center, Mississippi

Agriculture in both terrestrial and space-controlled environments relies heavily on artificial illumination for efficient photosynthesis. Plant-growth illumination systems require high photon flux in the spectral range corresponding with plant photosynthetic active radiation (PAR) (400–700 nm), high spatial uniformity to promote uniform growth, and high energy efficiency to minimize electricity usage. The proposed plant-growth system takes advantage of the highly diffuse reflective surfaces on the interior of a sphere, hemisphere, or other nearly enclosed structure that is coated with highly reflective materials. This type of surface and structure uniformly mixes discrete light sources to produce highly uniform illumination. Multiple reflections from within the dome-like structures are exploited to obtain diffuse illumination, which promotes the efficient reuse of photons that have not yet been absorbed by plants. The highly reflective surfaces encourage only the plant tissue (placed inside the sphere or enclosure) to absorb the light. Discrete light sources, such as light emitting diodes (LEDs), are typically used because of their high efficiency, wavelength selection, and electronically dimmable properties. The light sources are arranged to minimize shadowing and to improve uniformity. Different wavelengths of LEDs (typically blue, green, and red) are used for photosynthesis. Wavelengths outside the PAR range can be added for plant diagnostics or for growth regulation (see figure).

The advantage of this approach over previous artificial illumination methods is that it facilitates the use of a few discrete point light sources to illuminate an extended plant volume/surface area while minimizing canopy shadow effects and providing nearly perfect uniform illumination. The lighting system method efficiently mixes light, recycles photons, and enables nearly 100 percent spatial mixing of various colors. This system also makes it possible to conduct plant-

growth research in diffuse light fields with various spectral distributions. In theory, this efficient mixing of different light sources, as well as the spatial uniformity enabled by the dome/hemisphere environment, should minimize plant-growth variability and optimize growth.

This work was done by George May of the Institute for Technology Development and Robert Ryan of Science Systems and Applications, Inc. for Stennis Space Center.

Inquiries concerning rights for the commercial use of this invention should be addressed to:

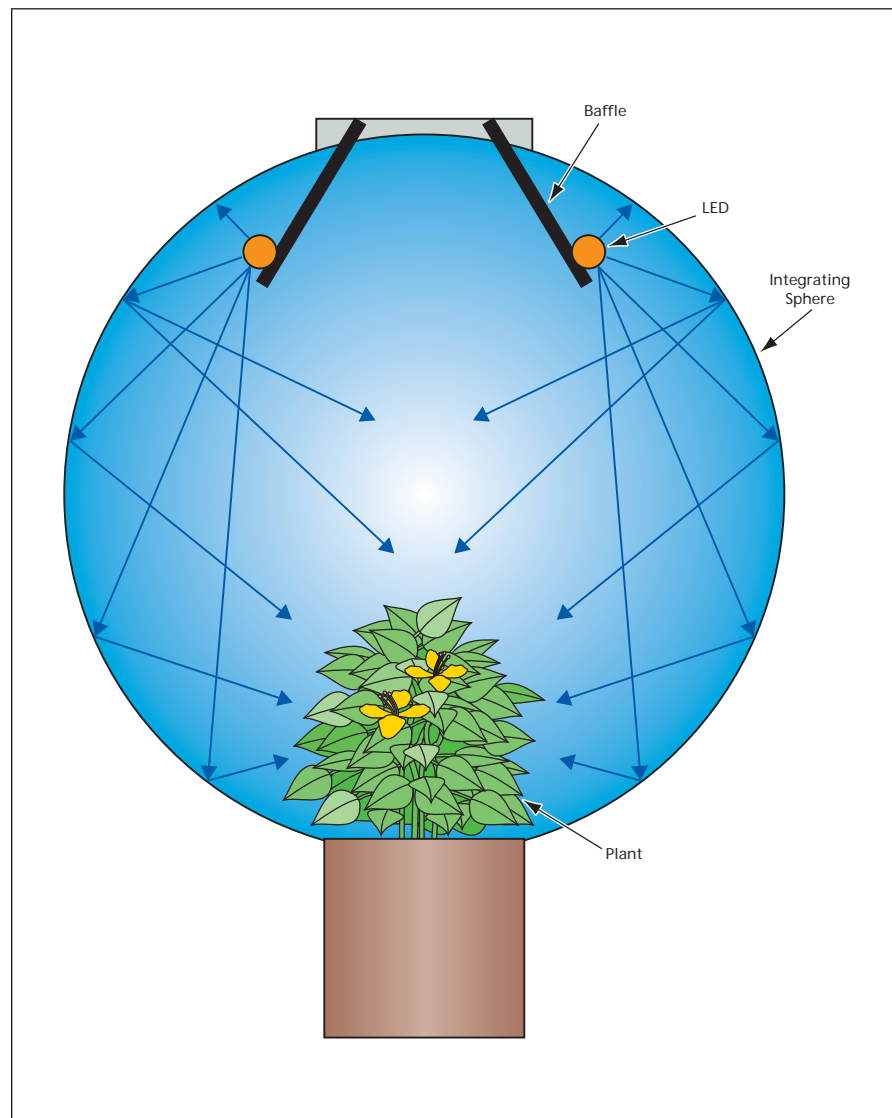
*Institute for Technology Development
Building 1103, Suite 118*

Stennis Space Center, MS 39529

Phone No.: (228) 688-2509

E-mail: gmay@iftid.org

Refer to SSC-00272, volume and number of this NASA Tech Briefs issue and the page number.



Multiple Diffuse Reflections mix light from several LEDs to illuminate plants diffusely at several wavelengths.

Microwave Plasma Hydrogen Recovery System

This method can efficiently recover hydrogen from natural gas.

Marshall Space Flight Center, Alabama

A microwave plasma reactor was developed for the recovery of hydrogen contained within waste methane produced by Carbon Dioxide Reduction Assembly (CRA), which reclaims oxygen from CO₂. Since half of the H₂ reductant used by the CRA is lost as CH₄, the ability to reclaim this valuable resource will simplify supply logistics for long-term manned missions. Microwave plasmas provide an extreme thermal environment within a very small and precisely controlled region of space, resulting in very high energy densities at low overall power, and thus can drive high-temperature reactions using equipment that is smaller, lighter, and less power-consuming than traditional fixed-bed and fluidized-bed catalytic reactors. The high energy density provides an economical means to conduct endothermic reactions that become

thermodynamically favorable only at very high temperatures.

Microwave plasma methods were developed for the effective recovery of H₂ using two primary reaction schemes: (1) methane pyrolysis to H₂ and solid-phase carbon, and (2) methane oligomerization to H₂ and acetylene. While the "carbon problem" is substantially reduced using plasma methods, it is not completely eliminated. For this reason, advanced methods were developed to promote CH₄ oligomerization, which recovers a maximum of 75 percent of the H₂ content of methane in a single reactor pass, and virtually eliminates the carbon problem. These methods were embodied in a prototype H₂ recovery system capable of sustained high-efficiency operation.

NASA can incorporate the innovation into flight hardware systems for

deployment in support of future long-duration exploration objectives such as a Space Station retrofit, Lunar outpost, Mars transit, or Mars base. The primary application will be for the recovery of hydrogen lost in the Sabatier process for CO₂ reduction to produce water in Exploration Life Support systems. Secondly, this process may also be used in conjunction with a Sabatier reactor employed to stockpile life-support oxygen as well as propellant and fuel production from Martian atmospheric CO₂.

This work was done by James Atwater, Richard Wheeler, Jr., Roger Dahl, and Neal Hadley of Umpqua Research Co. for Marshall Space Flight Center. For more information, contact Sammy Nabors, MSFC Commercialization Assistance Lead, at sammy.a.nabors@nasa.gov. Refer to MFS-32769-1.



Producing Hydrogen by Plasma Pyrolysis of Methane

Plasma pyrolysis offers several advantages over traditional catalytic pyrolysis.

Marshall Space Flight Center, Alabama

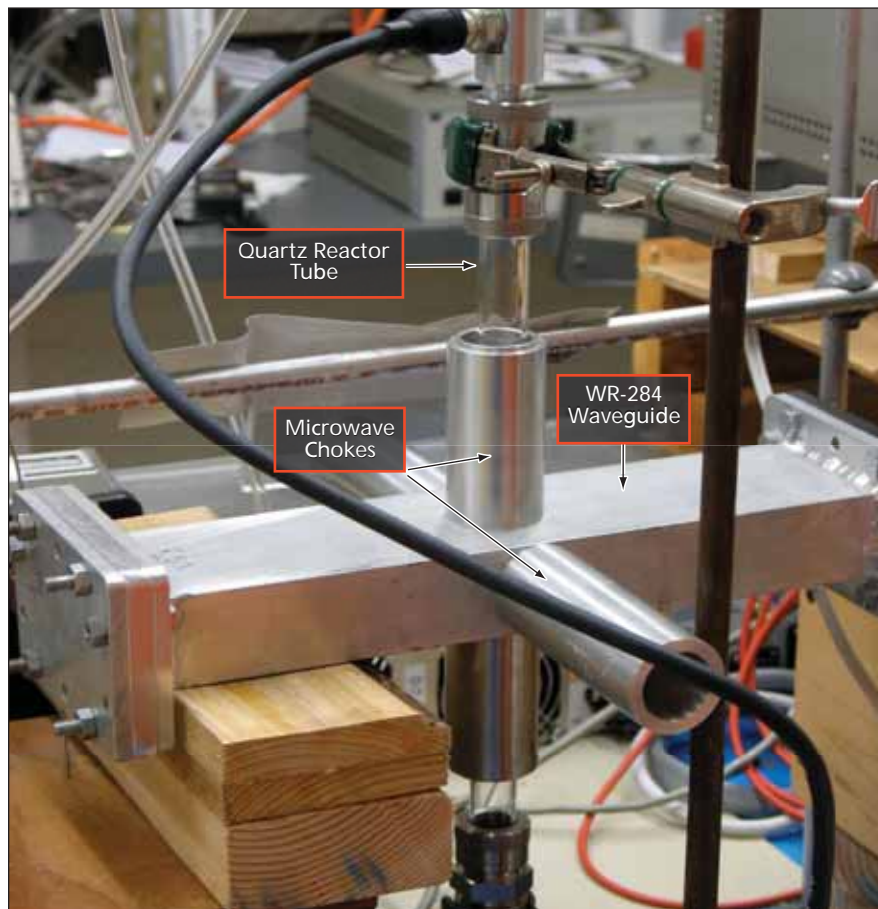
Plasma pyrolysis of methane has been investigated for utility as a process for producing hydrogen. This process was conceived as a means of recovering hydrogen from methane produced as a byproduct of operation of a life-support system aboard a spacecraft. On Earth, this process, when fully developed, could be a means of producing hydrogen (for use as a fuel) from methane in natural gas.

The most closely related prior competing process — catalytic pyrolysis of methane — has several disadvantages:

- The reactor used in the process is highly susceptible to fouling and deactivation of the catalyst by carbon deposits, necessitating frequent regeneration or replacement of the catalyst.
- The reactor is highly susceptible to plugging by deposition of carbon within fixed beds, with consequent channeling of flow, high pressure drops, and severe limitations on mass transfer, all contributing to reductions in reactor efficiency.
- Reaction rates are intrinsically low.
- The energy demand of the process is high.

In contrast, because the plasma pyrolysis process does not involve either a catalyst or fixed beds, it is inherently amenable to long-term, continuous operation without fouling of a catalyst or plugging of beds. Also, because this process involves only minimal heating of non-reactive components, it offers potential advantages of operation at relatively low power with high energy efficiency, plus enhanced safety (because of lower power levels and fewer hot surfaces).

The apparatus used in the investigation includes a 0.75-in. (1.9-cm)-diameter quartz reactor tube that contains the methane feed gas. Part of the length of the reactor tube lies in a horizontal WR-284 rectangular waveguide (see figure), through which microwave power is supplied to excite the methane to the plasma state. The reactor tube is inserted vertically through the middle of the horizontal waveguide via vertical



The **Quartz Reactor Tube** is inserted vertically through the middle of the horizontal WR-284 waveguide. In the portion of the tube that lies inside the waveguide, methane contained in the tube is excited to plasma by microwave power.

metal tubes, attached to the waveguide, that serve as microwave chokes. Apertures defined by two additional, horizontally oriented microwave chokes enable direct visual observation of the plasma. The microwave system delivers variable microwave power levels, monitors delivered and reflected power, and enables matching of microwave-source, waveguide, and load impedances (the main load being the plasma) for maximum power-transmission efficiency. The microwave source is a water-cooled magnetron that operates at the fixed frequency of 2.45 GHz and can deliver between 100 and 1,200 Watts of power under manual or computer control. Re-

flected microwave power not absorbed by the plasma is absorbed by a circulating-water load.

In operation, a process gas that consists of or includes methane is fed into the reactor through a mass flow controller that has a range from 0 to 1,000 standard cubic centimeters per minute. The microwave plasma is created and confined within the portion of the quartz tube that lies inside the waveguide. Early experiments were conducted using a 1:9 methane:argon feed-gas mixture, followed by experiments using pure methane. Operating conditions were identified under which methane-to-hydrogen conversion efficiencies ap-

proached 100 percent. Long-term tests were conducted to demonstrate continuous production of hydrogen without loss of reactor efficiency. Chemical analyses of the reaction products revealed that generation of hydrogen through decomposition of methane is accompanied by a

combination of cracking, oligomerization, and aromatization reactions, which tend to minimize the formation of elemental carbon. Further research is planned to refine understanding of these reactions and to determine whether and how they might be exploited.

This work was done by James Atwater, James Akse, and Richard Wheeler of Umpqua Research Co. for Marshall Space Flight Center. For further information, contact Sammy Nabors, MSFC Commercialization Assistance Lead, at sammy.a.nabors@nasa.gov. Refer to MFS-32539-1.

Self-Deployable Membrane Structures

These support structures can be used as portable shelters, camping tents, and thermal insulation.

NASA's Jet Propulsion Laboratory, Pasadena, California

Currently existing approaches for deployment of large, ultra-lightweight gossamer structures in space rely typically upon electromechanical mechanisms and mechanically expandable or inflatable booms for deployment and to maintain them in a fully deployed, operational configuration. These support structures, with the associated deployment mechanisms, launch restraints, inflation systems, and controls, can comprise more than 90 percent of the total mass budget. In addition, they significantly increase the stowage volume, cost, and complexity.

A CHEM (cold hibernated elastic memory) membrane structure without any deployable mechanism and support booms/structure is deployed by using shape memory and elastic recovery. The use of CHEM micro-foams reinforced with carbon nanotubes is considered for thin-membrane structure applications. In this advanced structural concept, the CHEM membrane structure is warmed up to allow packaging and stowing prior to launch, and then cooled to induce hibernation of the internal restoring forces. In space, the membrane remembers its original shape and size when warmed up. After the internal restoring forces deploy the structure, it is then cooled to achieve rigidization. For this

type of structure, the solar radiation could be utilized as the heat energy used for deployment and space ambient temperature for rigidization.

The overall simplicity of the CHEM self-deployable membrane is one of its greatest assets. In present approaches to space-deployable structures, the stowage and deployment are difficult and challenging, and introduce a significant risk, heavy mass, and high cost. Simple procedures provided by CHEM membrane greatly simplify the overall end-to-end process for designing, fabricating, deploying, and rigidizing large structures. The CHEM membrane avoids the complexities associated with other methods for deploying and rigidizing structures by eliminating deployable booms, deployment mechanisms, and inflation and control systems that can use up the majority of the mass budget.

In addition, highly integrated multifunctional CHEM membranes with embedded thin-film electronics, sensors, actuators, and power sources could be used to perform other spacecraft functions such as a communication, navigation, science gathering, and power generation.

This advanced membrane concept represents the introduction of a new generation of self-deployable structures.

This technology will introduce a new paradigm for defining configurations for space-based structures and for defining future mission architectures. It will provide new standards for fabricating, stowing, deploying, and rigidizing large deployable structures in a simple, straightforward process.

A number of deployable structures are used for space robotics and other support deployable structures for solar sails, telecommunication, power, sensing, thermal control, impact, and radiation protection systems. A self-deployable membrane structure could be used on some of these space applications with a big improvement.

Although the space community is the major beneficiary, potential commercial applications are foreseen for this technology. It could be applied to deployable shelters, storage places, and camping tents. Other potential applications are seen in self-deployable house construction, thermal insulation, automotive, packaging, and biomedical.

This work was done by Witold M. Sokolowski and Paul B. Willis of Caltech and Seng C. Tan of Wright Materials Research Co. for NASA's Jet Propulsion Laboratory. For more information, contact iaoffice@jpl.nasa.gov. NPO-41759

Reactivation of a Tin-Oxide-Containing Catalyst

This technique extends the lifetime of a catalyst in a laser discharge.

Langley Research Center, Hampton, Virginia

The electrons in electric-discharge CO₂ lasers cause dissociation of some CO₂ into O₂ and CO, and attach themselves to electronegative molecules such as O₂, forming negative O₂ ions, as well as larger negative ion clusters by colli-

sions with CO or other molecules. The decrease in CO₂ concentration due to dissociation into CO and O₂ will reduce the average repetitively pulsed or continuous wave laser power, even if no disruptive negative ion instabilities occur. Ac-

cordingly, it is the primary object of this invention to extend the lifetime of a catalyst used to combine the CO and O₂ products formed in a laser discharge.

A promising low-temperature catalyst for combining CO and O₂ is platinum

on tin oxide (Pt/SnO₂). First, the catalyst is pretreated by a standard procedure. The pretreatment is considered complete when no measurable quantity of CO₂ is given off by the catalyst. After this standard pretreatment, the catalyst is ready for its low-temperature use in the sealed, high-energy, pulsed CO₂ laser. However, after about 3,000 minutes of operation, the activity of the catalyst begins to slowly diminish. When the catalyst experiences diminished activity during exposure to the circulating gas stream inside or external to the laser, the heated zone surrounding the catalyst is raised to a temperature between 100 and 400 °C. A temperature of 225 °C was experimentally found to provide an ade-

quate temperature for reactivation. During this period, the catalyst is still exposed to the circulating gas inside or external to the laser.

This constant heating and exposing the catalyst to the laser gas mixture is maintained for an hour. After heating and exposing for an appropriate amount of time, the heated zone around the catalyst is allowed to return to the nominal operating temperature of the CO₂ laser. This temperature normally resides in the range of 23 to 100 °C.

Catalyst activity can be measured as the percentage conversion of CO to CO₂. In the specific embodiment described above, the initial steady-state conversion percentage was 70 percent. After four

days, this conversion percentage decreased to 67 percent. No decrease in activity is acceptable because the catalyst must maintain its activity for long periods of time. After being subjected to the reactivation process of the present invention, the conversion percentage rose to 77 percent. Such a reactivation not only returned the catalyst to its initial steady state but resulted in a 10-percent improvement over the initial steady state value.

This work was done by Robert Hess, Barry Sidney, David Schryer, Irvin Miller, George Miller, Bill Upchurch, and Patricia Davis of Langley Research Center and Kenneth Brown of Old Dominion University. Further information is contained in a TSP (see page 1). LAR-13845-1



Functionalization of Single-Wall Carbon Nanotubes by Photo-Oxidation

John H. Glenn Research Center, Cleveland, Ohio

A new technique for carbon nanotube oxidation was developed based upon the photo-oxidation of organic compounds. The resulting method is more benign than conventional oxidation approaches and produces single-wall carbon nanotubes (SWCNTs) with higher levels of oxidation.

In this procedure, an oxygen saturated suspension of SWNTs in a suitable solvent containing a singlet oxygen sensitizer, such as Rose Bengal, is irradiated with ultraviolet light. The resulting oxidized tubes are recovered by filtering

the suspension, followed by washing to remove any adsorbed solvent and sensitizer, and drying in a vacuum oven. Chemical analysis by FT-infrared and x-ray photoelectron spectroscopy revealed that the oxygen content of the photo-oxidized SWCNT was 11.3 atomic % compared to 6.7 atomic % for SWCNT that had been oxidized by standard treatment in refluxing acid.

The photo-oxidized SWCNT produced by this method can be used directly in various polymer matrixes, or can be further modified by chemical reactions at

the oxygen functional groups and then used as additives. This method may also be suitable for use in oxidation of multi-wall carbon nanotubes and graphenes.

This work was done by Marisabel Lebron-Colon and Michael A. Meador for Glenn Research Center. Further information is contained in a TSP (see page 1).

Inquiries concerning rights for the commercial use of this invention should be addressed to NASA Glenn Research Center, Innovative Partnerships Office, Attn: Steve Fedor, Mail Stop 4-8, 21000 Brookpark Road, Cleveland, Ohio 44135. Refer to LEW-18542-1.



Miniature Piezoelectric Macro-Mass Balance

This system can be used to verify the mass of multiple samples in pharmaceutical and food-processing applications.

NASA's Jet Propulsion Laboratory, Pasadena, California

Mass balances usually use a strain gauge that requires an impedance measurement and is susceptible to noise and thermal drift. A piezoelectric balance can be used to measure mass directly by monitoring the voltage developed across the piezoelectric balance, which is linear with weight or it can be used in resonance to produce a frequency change proportional to the mass change (see figure). The piezoelectric actuator/balance is swept in frequency through its fundamental resonance. If a small mass is added to the balance, the resonance frequency shifts down in proportion to the mass. By monitoring the frequency shift, the mass can be determined.

This design allows for two independent measurements of mass. Additionally, more than one sample can be verified because this invention allows for each sample to be transported away from the measuring device upon completion of the measurement, if required.

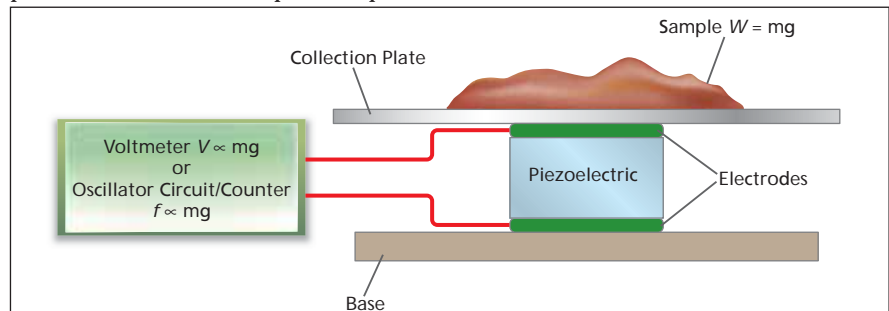
A piezoelectric actuator, or many piezoelectric actuators, was placed between the collection plate of the sampling system and the support structure. As the sample mass is added to the plate, the piezoelectrics are stressed, causing them to produce a voltage that is proportional to the mass and acceleration. In addition, a change in mass Δm pro-

duces a change in the resonance frequency with Δf proportional to Δm . In a microgravity environment, the spacecraft could be accelerated to produce a force on the piezoelectric actuator that would produce a voltage proportional to the mass and acceleration. Alternatively, the acceleration could be used to force the mass on the plate, and the inertial effects of the mass on the plate would produce a shift in the resonance frequency with the change in frequency related to the mass change.

Three prototypes of the mass balance mechanism were developed. These macro-mass balances each consist of a solid base and an APA 60 Cedrat flextensional piezoelectric actuator supporting a measuring plate. A similar structure with 3 APA 120 Cedrat flextensional piezoelectric actuators spaced equidis-

tantly at 120° supporting the plate and a softer macro balance with an APA 150 actuator/sensor were developed. These flextensional actuators were chosen because they increase the sensitivity of the actuator to stress, allow the piezoelectric to be pre-stressed, and the piezoelectric element is a stacked multilayer actuator, which has a considerably lower input impedance than a monolithic element that allows for common instruments (e.g., input impedance of 10 megohms) to measure the voltage without rapidly discharging the charge/voltage on the piezoelectric actuator.

This work was done by Stewart Sherrit, Ashitey Trebi-Ollennu, Robert G. Bonitz, and Yoseph Bar-Cohen of Caltech for NASA's Jet Propulsion Laboratory. For more information, contact iaoffice@jpl.nasa.gov. NPO-47161



There are Two Methods of Measuring Mass: A direct method uses a voltmeter; an indirect method uses an oscillator circuit/counter.

Acoustic Liner for Turbomachinery Applications

This acoustic liner reduces turbomachinery noise of aircraft.

John H. Glenn Research Center, Cleveland, Ohio

The purpose of this innovation is to reduce aircraft noise in the communities surrounding airports by significantly attenuating the noise generated by the turbomachinery, and enhancing safety by providing a containment barrier for a blade failure. Acoustic liners are used in today's turbofan engines to reduce noise. The amount of noise re-

duction from an acoustic liner is a function of the treatment area, the liner design, and the material properties, and limited by the constraints of the nacelle or casement design. It is desirable to increase the effective area of the acoustic treatment to increase noise suppression. Modern turbofan engines use "wide-chord" rotor blades, which means

there is considerable treatment area available over the rotor tip.

Turbofan engines require containment over the rotors for protection from blade failure. Traditional methods use a material wrap such as Kevlar integrated with rub strips and sometimes metal layers (sandwiches). It is possible to substitute the soft rub-strip

material with an open-cell metallic foam that provides noise-reduction benefits and a sacrificial material in the first layer of the containment system.

An open-cell foam was evaluated that behaves like a bulk acoustic liner, serves as a tip rub strip, and can be integrated with a rotor containment system. Foams can be integrated with the fan-containment system to provide sufficient safety margins and increased noise attenuation. The major innovation is the integration of the foam with the containment.

The uniqueness of the innovation is the ability to reduce turbomachinery noise for aircraft engine applications while providing sufficient blade containment and minimal (if any) aerody-

amic penalty. The innovation can be applied to compressors, turbines, and fans. Space is usually limited over the rotors due to the need for containment systems. The innovation replaces the first layer of the containment system with a foam that behaves like an acoustic bulk liner. The material properties of the foam can be tailored for temperature, density, porosity, and weight to suit the application. Existing turbofan engines do not use acoustic treatment placed directly over the rotor. The innovation enables this due to the foam behaving like a rub strip and an acoustic liner. Full-scale testing of production turbofan engine resulted in 5-dB total attenuation.

This innovation can be applied to other turbomachinery where noise reduction is needed from the rotors; for example, ground power systems, cooling/ventilating fans, and ducted propellers.

This work was done by Dennis L. Huff and Daniel L. Sutliff of Glenn Research Center; Michael G. Jones of Langley Research Center; and Mohan G. Hebsur of the Ohio Space Institute. Further information is contained in a TSP (see page 1).

Inquiries concerning rights for the commercial use of this invention should be addressed to NASA Glenn Research Center, Innovative Partnerships Office, Attn: Steve Fedor, Mail Stop 4-8, 21000 Brookpark Road, Cleveland, Ohio 44135. Refer to LEW-18438-1.

Metering Gas Strut for Separating Rocket Stages

Marshall Space Flight Center, Alabama

A proposed gas strut system would separate a liquid-fueled second rocket stage from a solid-fueled first stage using an array of pre-charged struts. The strut would be a piston-and-cylinder mechanism containing a compressed gas. Adiabatic expansion of the gas would drive the extension of the strut. The strut is designed to produce a force-versus-time profile, chosen to prevent agitation of the liquid fuel, in which the force would increase from an initial low value to a peak value, then decay toward the end of the stroke.

The strut would include a piston chamber and a storage chamber. The piston chamber would initially contain gas at a low pressure to provide the initial low separation force. The storage chamber would contain gas at a higher pressure. The piston would include a longitudinal metering rod containing an array of small holes, sized to restrict the flow gas between the chambers, that would initially not be exposed to the interior of the piston chamber. During subsequent expansion, the piston mo-

tion would open more of the metering holes between the storage and piston chambers, thereby increasing the flow of gas into the piston chamber to produce the desired buildup of force.

This work was done by Brian Floyd of Integrated Concepts Research Corp. for Marshall Space Flight Center. For further information, contact Sammy Nabors, MSFC Commercialization Assistance Lead, at sammy.a.nabors@nasa.gov. Refer to MFS-32660-1.

Large-Flow-Area Flow-Selective Liquid/Gas Separator

A two-phase flow separator for fuel cells operates between 2 and 10 kW in multi-g environments.

Lyndon B. Johnson Space Center, Houston, Texas

This liquid/gas separator provides the basis for a first stage of a fuel cell product water/oxygen gas phase separator. It can separate liquid and gas in bulk in multiple gravity environments. The system separates fuel cell product water entrained with circulating oxygen gas from the outlet of a fuel cell stack before allowing the gas to return to the fuel cell stack inlet. Additional makeup oxygen gas is added either before or after the separator to account for the gas consumed in the fuel cell power plant. A large volume is provided upstream of porous material in the separator to allow for the collection of water that does not exit the separator with the

outgoing oxygen gas. The water then can be removed as it continues to collect, so that the accumulation of water does not impede the separating action of the device.

The system is designed with a series of tubes of the porous material configured into a shell-and-tube heat exchanger configuration. The two-phase fluid stream to be separated enters the shell-side portion of the device. Gas flows to the center passages of the tubes through the porous material and is then routed to a common volume at the end of the tubes by simple pressure difference from a pumping device. Gas flows through the porous material of the

tubes with greater ease as a function of the ratio of the dynamic viscosity of the water and gas. By careful selection of the dimensions of the tubes (wall thickness, porosity, diameter, length of the tubes, number of the tubes, and tube-to-tube spacing in the shell volume) a suitable design can be made to match the magnitude of water and gas flow, developed pressures from the oxygen reactant pumping device, and required residual water inventory for the shell-side volume.

The system design has the flexibility to be configured in a few different ways. Special configurations of the tube geometry could aid the operation of the re-

quired second stage to manage the continual accumulation of water in the shell-side volume. An example would be with the circularization of the tubes so that water would tend to be swirled or slung to the outside of the tube bundle for subsequent removal by a second stage of the separator intended for the fine separation of remaining gas from the product water stream before it exits the separator. Another version could in-

clude in-separator reactant pressure regulation, ejector-based reactant pumping, and reactant pre-humidifying thermal control through the use of in-separator thermal conditioning.

The system has few moving parts and is not subject to degradation of performance due to changes in material properties (surface wetting characteristics, etc.). The design eliminates the possibility of flooding of the fuel cell stack dur-

ing nominal operations, reduces the complexity of the task of maintaining the residual water volume of the separator during periods of non-use of the fuel cell power system, and can be packaged in a manner suitable for spacecraft fuel cell power systems.

This work was done by Arturo Vasquez and Karla F. Bradley for Johnson Space Center. Further information is contained in a TSP (see page 1). MSC-24157-1.

⚙️ Counterflowing Jet Subsystem Design

Marshall Space Flight Center, Alabama

A counterflowing jet design (a spacecraft and trans-atmospheric subsystem) employs centrally located, supersonic cold gas jets on the face of the vehicle, ejecting into the oncoming free stream. Depending on the supersonic free-stream conditions and the ejected mass flow rate of the counterflowing jets, the bow shock of the vehicle is moved upstream, further

away from the vehicle. This results in an increasing shock standoff distance of the bow shock with a progressively weaker shock. At a critical jet mass flow rate, the bow shock becomes so weak that it is transformed into a series of compression waves spread out in a much wider region, thus significantly modifying the flow that wets the outer surfaces, with an attendant

reduction in wave and skin friction drag and aerothermal loads.

This work was done by Rebecca Farr, Endwell Daso, Victor Pritchett, and Ten-See Wang of Marshall Space Flight Center. For more information, contact Sammy Nabors, MSFC Commercialization Assistance Lead, at sammy.a.nabors@nasa.gov. Refer to MFS-32604-1.

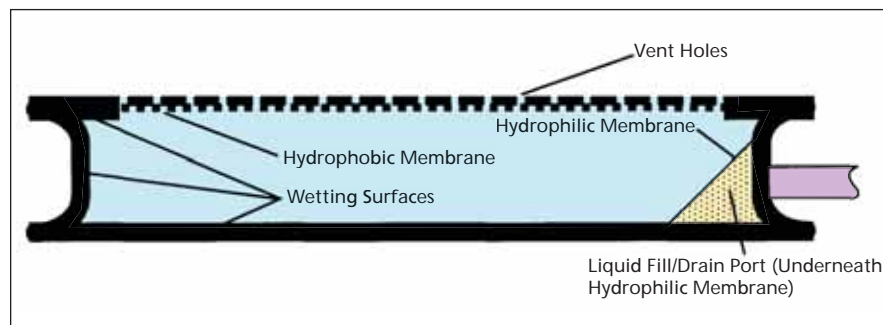
⚙️ Water Tank With Capillary Air/Liquid Separation

Tank is filled and emptied as needed in microgravity.

Lyndon B. Johnson Space Center, Houston, Texas

A bladderless water tank (see figure) has been developed that contains capillary devices that allow it to be filled and emptied, as needed, in microgravity. When filled with water, the tank shields human occupants of a spacecraft against cosmic radiation. A membrane that is permeable by air but is hydrophobic (neither wettable nor permeable by liquid water) covers one inside surface of the tank. Grooves between the surface and the membrane allow air to flow through vent holes in the surface as the tank is filled or drained. A margin of wettable surface surrounds the edges of the membrane, and all the other inside tank surfaces are also wettable. A fill/drain port is located in one corner of the tank and is covered with a hydrophilic membrane.

As filling begins, water runs from the hydrophilic membrane into the corner fillets of the tank walls. Continued filling in the absence of gravity will result in a



This functional schematic shows key components of the Radiation-Shield Water Tank.

single contiguous air bubble that will be vented through the hydrophobic membrane. The bubble will be reduced in size until it becomes spherical and smaller than the tank thickness. Draining the tank reverses the process. Air is introduced through the hydrophobic membrane, and liquid continuity is maintained with the fill/drain port through the corner fillets. Even after the

tank is emptied, as long as the suction pressure on the hydrophilic membrane does not exceed its bubble point, no air will be drawn into the liquid line.

This work was done by Eugene K. Ungar, Frederick Smith, and Gregg Edeen of Johnson Space Center and Jay C. Almlie of Hernandez Engineering, Inc. Further information is contained in a TSP (see page 1). MSC-23251-1



True Shear Parallel Plate Viscometer

This instrument is designed to measure the viscosity of non-Newtonian liquids.

Marshall Space Flight Center, Alabama

This viscometer (which can also be used as a rheometer) is designed for use with liquids over a large temperature range. The device consists of horizontally disposed, similarly sized, parallel plates with a precisely known gap. The lower plate is driven laterally with a motor to apply shear to the liquid in the gap. The upper plate is freely suspended from a double-arm pendulum with a sufficiently long radius to reduce height variations during the swing to negligible levels. A sensitive load cell measures the shear force applied by the liquid to the upper plate. Viscosity is measured by taking the ratio of shear stress to shear rate.

The bearing points of the suspended plate and the upper arms of the pendulum ensure any motion is constrained to one axis, and no friction or resistance from the apparatus contributes to the load. Unlike other viscometers, e.g., those using rotating cylinders or disks, this design follows the simplest mechanical model to measure viscosity. By using large vitreous quartz plates and small gaps, liquids with very low viscosities at low temperatures can be measured with

the same tooling as viscous liquids, like glass at elevated temperatures. By maintaining a constant gap and driving the lower plate with a linear driver motor, the liquid between the plates undergoes a uniform amount, and therefore rate, of shear over its volume.

When using the vitreous quartz plates to contain the liquid, high-temperature operation up to 800 °C, or more, can be considered. The transparency of the plates permits a precise measure of the liquid area of contact on the plate with a camera or similar method. One can recover the gap dimension from knowledge of the liquid area and the amount of liquid volume used; alternatively, one can set the gap and measure the area of spread to determine the liquid volume if it is an arbitrary amount. Another advantage of this method is the ability to quickly adjust the gap, and to determine what it is precisely (from the liquid spread area) between measurements of viscosity.

Although not implemented in the prototype, the plates can be temperature-controlled to ensure the liquid in

contact with them is at proper temperatures. By building heaters and temperature sensors into the plates, one can be certain the liquid in contact will have the proper temperature. The thickly spread liquid will respond to the substrate (heater plate) temperature very rapidly. The thermal lag will be confined to the heater plates themselves, but not to support structures or fixtures.

The pendulum mounting of the upper plate offers noise elimination because only the lateral shear force is read on the load cell. The fixture and sample mass do not interfere with the load measurement. Furthermore, particularly worthwhile with viscous glasses, only small displacements away from the rest position of the pendulum are required to make a measurement. This reduces instrument error to a minimum.

This work was done by Edwin Ethridge of Marshall Space Flight Center and William Kaukler of the University of Alabama, Huntsville. For more information, contact Sammy Nabors, MSFC Commercialization Assistance Lead, at sammy.a.nabors@nasa.gov. Refer to MFS-32558-1.

Focusing Diffraction Grating Element With Aberration Control

The device has application in spectrometers, optical processors, and remote sensors.

Goddard Space Flight Center, Greenbelt, Maryland

Diffraction gratings are optical components with regular patterns of grooves, which angularly disperse incoming light by wavelength in a single plane, called dispersion plane. Traditional gratings on flat substrates do not perform wavefront transformation in the plane perpendicular to the dispersion plane. The device proposed here exhibits regular diffraction grating behavior, dispersing light. In addition, it performs wavelength transformation (focusing or defocusing) of diffracted light in a direction perpendicular to the dispersion plane (called sagittal plane).

The device is composed of a diffraction grating with the grooves in the form of equidistant arcs. It may be formed by defining a single arc or an arc approximation, then translating it along a certain direction by a distance equal to a multiple of a fixed distance ("grating period") to obtain other groove positions. Such groove layout is nearly impossible to obtain using traditional ruling methods, such as mechanical ruling or holographic scribing, but is trivial for lithographically scribed gratings. Lithographic scribing is the newly developed method first commercially introduced by LightSmyth Tech-

nologies, which produces gratings with the highest performance and arbitrary groove shape/spacing for advanced aberration control. Unlike other types of focusing gratings, the grating is formed on a flat substrate. In a plane perpendicular to the substrate and parallel to the translation direction, the period of the grating and, therefore, the projection of its k -vector onto the plane is the same for any location on the grating surface. In that plane, no waveform transformation by the grating k -vector occurs, except of simple redirection.

Therefore, diffracted light experiences no wavelength transformation

in the dispersion plane. It is redirected in much the same way as with a flat mirror. However, in the sagittal plane light gets redirected in a manner similar to a cylindrical mirror. It exhibits focusing with the focal length only defined by the curvature of the grooves, the incident wavelength, and the grating period.

Because of this, one single diffraction grating can exhibit two dispersal patterns. It disperses light just like a regular flat diffraction grating, while at the same time focusing (or de-focusing) diffracted light onto a perpendicular plane. This focusing generates less aberrations than a mirror would. Non-trivial property of this device is

that its focal length for a fixed wavelength does not depend on the incident angle, even if the angle is extremely non-paraxial.

This work was done by Dmitri Iazikov, Thomas W. Mossberg, and Christoph M. Greiner of Goddard Space Flight Center. Further information is contained in a TSP (see page 1). GSC-15680-1

Universal Millimeter-Wave Radar Front End

NASA's Jet Propulsion Laboratory, Pasadena, California

A quasi-optical front end allows any arbitrary polarization to be transmitted by controlling the timing, amplitude, and phase of the two input ports. The front end consists of two independent channels — horizontal and vertical. Each channel has two ports — transmit and receive. The transmit signal is linearly polarized so as to pass through a periodic wire grid. It is then propagated through a ferrite Faraday rotator, which rotates the polarization state 45°. The received signal is propagated through the Faraday rotator in the opposite di-

rection, undergoing a further 45° of polarization rotation due to the non-reciprocal action of the ferrite under magnetic bias. The received signal is now polarized at 90° relative to the transmit signal. This signal is now reflected from the wire grid and propagated to the receive port.

The horizontal and vertical channels are propagated through, or reflected from, another wire grid. This design is an improvement on the state of the art in that any transmit signal polarization can be chosen in whatever sequence de-

sired. Prior systems require switching of the transmit signal from the amplifier, either mechanically or by using high-power millimeter-wave switches. This design can have higher reliability, lower mass, and more flexibility than mechanical switching systems, as well as higher reliability and lower losses than systems using high-power millimeter-wave switches.

This work was done by Raul M. Perez of Caltech for NASA's Jet Propulsion Laboratory. For more information, contact iaoffice@jpl.nasa.gov. NPO-46654

Mode Selection for a Single-Frequency Fiber Laser

NASA's Goddard Space Flight Center, Greenbelt, Maryland

A superstructured fiber-grating-based mode selection filter for a single-frequency fiber laser eliminates all free-space components, and makes the laser truly all-fiber. A ring cavity provides for stable operations in both frequency and power. There is no alignment or realignment required. After the fibers and components are spliced together and packaged, there is no need for specially trained technicians for operation or maintenance. It can be integrated with

other modules, such as telescope systems, without extra optical alignment due to the flexibility of the optical fiber.

The filter features a narrow line width of 1 kHz and side mode suppression ratio of 65 dB. It provides a high-quality laser for lidar in terms of coherence length and signal-to-noise ratio, which is 20 dB higher than solid-state or microchip lasers.

This concept is useful in material processing, medical equipment, biomedical

instrumentation, and optical communications. The pulse-shaping fiber laser can be directly used in space, airborne, and satellite applications including lidar, remote sensing, illuminators, and phase-array antenna systems.

This work was done by Jian Liu of Goddard Space Flight Center. For further information, contact the Goddard Innovative Partnerships Office at (301) 286-5810. GSC-15600-1

Qualification and Selection of Flight Diode Lasers for Space Applications

NASA's Jet Propulsion Laboratory, Pasadena, California

The reliability and lifetime of laser diodes is critical to space missions. The Nuclear Spectroscopic Telescope Array (NuSTAR) mission includes a metrology system that is based upon laser diodes. An operational test facility has

been developed to qualify and select, by mission standards, laser diodes that will survive the intended space environment and mission lifetime. The facility is situated in an electrostatic discharge (ESD) certified cleanroom and consist of an

enclosed temperature-controlled stage that can accommodate up to 20 laser diodes. The facility is designed to characterize a single laser diode, in addition to conducting laser lifetime testing on up to 20 laser diodes simultaneously.

A standard laser current driver is used to drive a single laser diode. Laser diode current, voltage, power, and wavelength are measured for each laser diode, and a method of selecting the most adequate laser diodes for space deployment is implemented. The method consists of creating histograms of laser threshold currents, powers at a designated current, and wavelengths at designated power. From these histograms, the laser diodes that illustrate a performance that is outside the normal are rejected and the re-

maining lasers are considered space-borne candidates.

To perform laser lifetime testing, the facility is equipped with 20 custom laser drivers that were designed and built by California Institute of Technology specifically to drive NuSTAR metrology lasers. The laser drivers can be operated in constant-current mode or alternating-current mode. Situated inside the enclosure, in front of the laser diodes, are 20 power-meter heads to record laser power throughout the duration of lifetime testing.

Prior to connecting a laser diode to the current source for characterization and lifetime testing, a background program is initiated to collect current, voltage, and resistance. This backstage data collection enables the operational test facility to have full laser diode traceability.

This work was done by Carl C. Liebe, Robert P. Dillon, Ivair Gontijo, Siamak Forouhar, Andrew A. Shapiro, Mark S. Cooper, and Patrick L. Meras of Caltech for NASA's Jet Propulsion Laboratory. For more information, contact iaoffice@jpl.nasa.gov. NPO-47164

Plenoptic Imager for Automated Surface Navigation

John H. Glenn Research Center, Cleveland, Ohio

An electro-optical imaging device is capable of autonomously determining the range to objects in a scene without the use of active emitters or multiple apertures. The novel, automated, low-power imaging system is based on a plenoptic camera design that was constructed as a breadboard system. Nanohmics proved feasibility of the concept by designing an optical system for a prototype plenoptic camera, developing simulated plenoptic images and range-calculation algorithms, constructing a breadboard proto-

type plenoptic camera, and processing images (including range calculations) from the prototype system.

The breadboard demonstration included an optical subsystem comprised of a main aperture lens, a mechanical structure that holds an array of micro lenses at the focal distance from the main lens, and a structure that mates a CMOS imaging sensor the correct distance from the micro lenses. The demonstrator also featured embedded electronics for camera readout, and a post-processor executing

image-processing algorithms to provide ranging information.

This work was done by Byron Zollars, Andrew Milder, and Michael Mayo of Nanohmics, Inc. for Glenn Research Center. Further information is contained in a TSP (see page 1).

Inquiries concerning rights for the commercial use of this invention should be addressed to NASA Glenn Research Center, Innovative Partnerships Office, Attn: Steve Fedor, Mail Stop 4-8, 21000 Brookpark Road, Cleveland, Ohio 44135. Refer to LEW-18525-1.

Maglev Facility for Simulating Variable Gravity

Effects of gravity on thermal fluid systems and small living things can be tested.

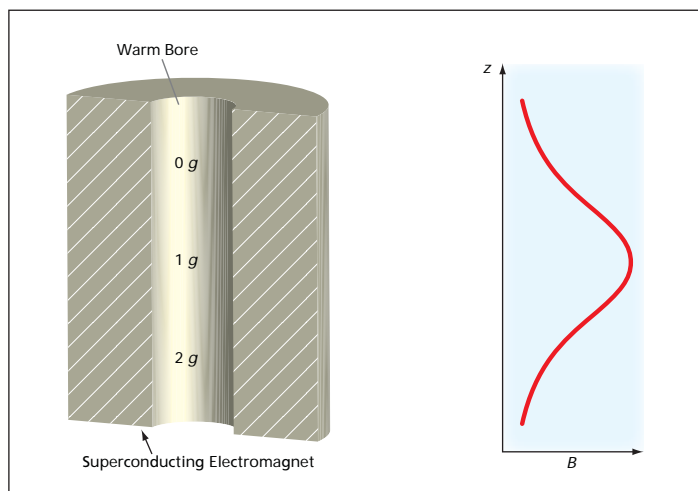
NASA's Jet Propulsion Laboratory, Pasadena, California

An improved magnetic levitation apparatus ("Maglev Facility") has been built for use in experiments in which there are requirements to impose variable gravity (including zero gravity) in order to assess the effects of gravity or the absence thereof on physical and physiological processes. The apparatus is expected to be especially useful for experiments on the effects of gravity on convection, boiling, and heat transfer in fluids and for experiments on mice to gain understanding of bone loss induced in human astronauts by prolonged exposure to reduced gravity in space flight.

The maglev principle employed by the apparatus is well established. The basic equation for equilibrium levitation of a diamagnetic object is

$$|\chi BV_z B / \mu_0| = \rho g,$$

where χ is the magnetic susceptibility of the object, B is the magnitude of the magnetic-flux density, μ_0 is the magnetic permeability of the vacuum, ρ is the mass density of the object, g is the local gravitational acceleration, and $\nabla_z B$ is the vertical gradient of the magnetic field. Diamagnetic cryogenic fluids such as liquid helium have been magnetically levitated for studying their phase transitions and critical



The Superconducting Electromagnet generates a static magnetic field with a vertical gradient. For water or other substances of diamagnetism, the gradient magnetic field opposes or aids the gravitational body force by an amount that varies with position along the bore.

behaviors. Biological entities consist mostly of diamagnetic molecules (e.g., water molecules) and thus can be levitated by use of sufficiently strong magnetic fields having sufficiently strong vertical gradients.

The heart of the present maglev apparatus is a vertically oriented superconducting solenoid electromagnet (see figure) that generates a static magnetic field of about 16 T with a vertical gradient sufficient for levitation of water in normal Earth gravity. The electromagnet is enclosed in a Dewar flask having a

volume of 100 L that contains liquid helium to maintain superconductivity. The Dewar flask features a 66-mm-diameter warm bore, lying within the bore of the magnet, wherein experiments can be performed at room temperature. The warm bore is accessible from its top and bottom ends. The superconducting electromagnet is run in the persistent mode, in which the supercurrent and the magnetic field can be maintained for weeks with little decay, making this apparatus extremely cost and energy efficient to operate. In addition to water,

this apparatus can levitate several common fluids: liquid hydrogen, liquid oxygen, methane, ammonia, sodium, and lithium, all of which are useful, variously, as rocket fuels or as working fluids for heat transfer devices. A drop of water 45 mm in diameter and a small laboratory mouse have been levitated in this apparatus.

This work was done by Yuanming Liu, Donald M. Strayer, and Ulf E. Israelsson of Caltech for NASA's Jet Propulsion Laboratory. Further information is contained in a TSP (see page 1).NPO-45886

Hybrid AlGaN-SiC Avalanche Photodiode for Deep-UV Photon Detection

NASA's Goddard Space Flight Center, Greenbelt, Maryland

The proposed device is capable of counting ultraviolet (UV) photons, is compatible for inclusion into space instruments, and has applications as deep-UV detectors for calibration systems, curing systems, and crack detection. The device is based on a Separate Absorption and Charge Multiplication (SACM) structure. It is based on aluminum gallium nitride (AlGaN) absorber on a silicon carbide APD (avalanche photodiode). The AlGaN layer absorbs incident

UV photons and injects photogenerated carriers into an underlying SiC APD that is operated in Geiger mode and provides current multiplication via avalanche breakdown.

The solid-state detector is capable of sensing 100-to-365-nanometer wavelength radiation at a flux level as low as 6 photons/pixel/s. Advantages include, visible-light blindness, operation in harsh environments (e.g., high temperatures), deep-UV detection response,

high gain, and Geiger mode operation at low voltage. Furthermore, the device can also be designed in array formats, e.g., linear arrays or 2D arrays (micropixels inside a superpixel).

This work was done by Shahid Aslam, Federico A. Herrero, and John Sigwarth of Goddard Space Flight Center and Neil Goldsman and Akin Akturk of The University of Maryland. Further information is contained in a TSP (see page 1). GSC-15604-1

High-Speed Operation of Interband Cascade Lasers

NASA's Jet Propulsion Laboratory, Pasadena, California

Optical sources operating in the atmospheric window of 3–5 μm are of particular interest for the development of free-space optical communication link. It is more advantageous to operate the free-space optical communication link in 3–5- μm atmospheric transmission window than at the telecom wavelength of 1.5 μm due to lower optical scattering, scintillation, and background radiation. However, the realization of optical communications at the longer wavelength has encountered significant difficulties due to lack of adequate optical sources and detectors operating in the desirable wavelength regions.

Interband Cascade (IC) lasers are novel semiconductor lasers that have a great potential for the realization of high-power, room-temperature optical sources in the 3–5- μm wavelength region, yet no experimental work, until this one, was done on high-speed direct modulation of IC lasers. Here, high-speed interband cascade laser, operating at wavelength 3.0 μm , has been developed and the first direct measurement of the laser modulation bandwidth has been performed using a unique, high-speed quantum well infrared photodetector (QWIP). The developed laser has modulation bandwidth exceeding 3

GHz. This constitutes a significant increase of the IC laser modulation bandwidth over currently existing devices. This result has demonstrated suitability of IC lasers as a mid-IR light source for multi-GHz free-space optical communications links.

This work was done by Alexander Soibel, Cory J. Hill, Sam A. Keo, Malcom W. Wright, and William H. Farr of Caltech; Rui Q. Yang of the University of Oklahoma; and H.C. Liu of the Institute for Microstructural Science for NASA's Jet Propulsion Laboratory. For more information, contact iaoffice@jpl.nasa.gov. NPO-46738



3D GeoWall Analysis System for Shuttle External Tank Foreign Object Debris Events

This new system augments and optimizes existing 2D monitoring capabilities.

Stennis Space Center, Mississippi

An analytical, advanced imaging method has been developed for the initial monitoring and identification of foam debris and similar anomalies that occur post-launch in reference to the space shuttle's external tank (ET). Remote sensing technologies have been used to perform image enhancement and analysis on high-resolution, true-color images collected with the DCS 760 Kodak digital camera located in the right umbilical well of the space shuttle. Improvements to the camera, using filters, have added sharpness/definition to the image sets; however, image review/analysis of the ET has been limited by the fact that the images acquired by umbilical cameras during launch are two-dimensional, and are usually non-referenceable between frames due to rotation translation of the ET as it falls away from the space shuttle. Use of

stereo pairs of these images can enable strong visual indicators that can immediately portray depth perception of damaged areas or movement of fragments between frames is not perceivable in two-dimensional images.

A stereoscopic image visualization system has been developed to allow 3D depth perception of stereo-aligned image pairs taken from in-flight umbilical and handheld digital shuttle cameras. This new system has been developed to augment and optimize existing 2D monitoring capabilities. Using this system, candidate sequential image pairs are identified for transformation into stereo viewing pairs. Image orientation is corrected using control points (similar points) between frames to place the two images in proper X-Y viewing perspective. The images are then imported into the WallView stereo viewing software

package. The collected control points are used to generate a transformation equation that is used to re-project one image and effectively co-register it to the other image. The co-registered, oriented image pairs are imported into a WallView image set and are used as a 3D stereo analysis slide show. Multiple sequential image pairs can be used to allow forensic review of temporal phenomena between pairs. The observer, while wearing linear polarized glasses, is able to review image pairs in passive 3D stereo.

This work was done by Richard Brown, Science Systems and Applications, Inc., Andrew Navard of Computer Sciences Corp., and Joseph Spruce of Science Systems and Applications, Inc. for Stennis Space Center.

Inquiries concerning rights for the commercial use of this invention should be addressed to the Intellectual Property Manager at Stennis Space Center (228) 688-1929. SSC-00331

Charge-Spot Model for Electrostatic Forces in Simulation of Fine Particulates

More accurate results are obtained by assigning multiple charge spots to dust particles instead of one.

John H. Glenn Research Center, Cleveland, Ohio

The charge-spot technique for modeling the static electric forces acting between charged fine particles entails treating electric charges on individual particles as small sets of discrete point charges, located near their surfaces. This is in contrast to existing models, which assume a single charge per particle. The charge-spot technique more accurately describes the forces, torques, and moments that act on triboelectrically charged particles, especially image-charge forces acting near conducting surfaces.

The discrete element method (DEM) simulation uses a truncation range to limit the number of near-neighbor charge spots via a shifted and truncated

potential Coulomb interaction. The model can be readily adapted to account for induced dipoles in uncharged particles (and thus dielectrophoretic forces) by allowing two charge spots of opposite signs to be "created" in response to an external electric field. To account for virtual overlap during contacts, the model can be set to automatically scale down the effective charge in proportion to the amount of virtual overlap of the charge spots. This can be accomplished by mimicking the behavior of two real overlapping spherical charge clouds, or with other approximate forms.

The charge-spot method much more closely resembles real non-uniform sur-

face charge distributions that result from tribocharging than simpler approaches, which just assign a single total charge to a particle. With the charge-spot model, a single particle may have a zero net charge, but still have both positive and negative charge spots, which could produce substantial forces on the particle when it is close to other charges, when it is in an external electric field, or when near a conducting surface. Since the charge-spot model can contain any number of charges per particle, can be used with only one or two charge spots per particle for simulating charging from solar wind bombardment, or with several charge spots

for simulating triboelectric charging. Adhesive image-charge forces acting on charged particles touching conducting surfaces can be up to 50 times stronger if the charge is located in discrete spots on the particle surface instead of being distributed uniformly over the surface of the particle, as is assumed by most other models.

Besides being useful in modeling particulates in space and distant objects, this modeling technique is useful for electrophotography (used in copiers) and in simulating the effects of static charge in the pulmonary delivery of fine dry powders.

This work was done by Otis R. Walton and Scott M. Johnson of Grainflow Dynamics,

Inc. for Glenn Research Center. Further information is contained in a TSP (see page 1).

Inquiries concerning rights for the commercial use of this invention should be addressed to NASA Glenn Research Center, Innovative Partnerships Office, Attn: Steve Fedor, Mail Stop 4-8, 21000 Brookpark Road, Cleveland, Ohio 44135. Refer to LEW-18403-1.

▶ Hidden Statistics Approach to Quantum Simulations

This dynamic system could help in building quantum computers.

NASA's Jet Propulsion Laboratory, Pasadena, California

Recent advances in quantum information theory have inspired an explosion of interest in new quantum algorithms for solving hard computational (quantum and non-quantum) problems. The basic principle of quantum computation is that the quantum properties can be used to represent structure data, and that quantum mechanisms can be devised and built to perform operations with this data. Three basic “non-classical” properties of quantum mechanics — superposition, entanglement, and direct-product decomposability — were main reasons for optimism about capabilities of quantum computers that promised simultaneous processing of large masses of highly correlated data. Unfortunately, these advantages of quantum mechanics came with a high price. One major problem is keeping the components of the computer in a coherent state, as the slightest interaction with the external world would cause the system to decohere. That is why the hardware implementation of a quantum computer is still unsolved.

The basic idea of this work is to create a new kind of dynamical system that would preserve the main three properties of quantum physics — superposition, entanglement, and direct-product decomposability — while allowing one to measure its state variables using classical methods. In other words, such a system would reinforce the advantages and minimize limitations of both quantum and classical aspects.

Based upon a concept of hidden statistics, a new kind of dynamical system for simulation of Schrödinger equation is proposed. The system represents a modified Madelung version of Schrödinger equation. It preserves superposition, entanglement, and direct-product decomposability while allowing one to measure its state variables using classical methods. Such an optimal combination of characteristics is a perfect match for simulating quantum systems. The model includes a transitional component of quantum potential (that has been overlooked in previous treatment of the

Madelung equation). The role of the transitional potential is to provide a jump from a deterministic state to a random state with prescribed probability density. This jump is triggered by blow-up instability due to violation of Lipschitz condition generated by the quantum potential. As a result, the dynamics attains quantum properties on a classical scale. The model can be implemented physically as an analog VLSI-based (very-large-scale integration-based) computer, or numerically on a digital computer.

This work opens a way of developing fundamentally new algorithms for quantum simulations of exponentially complex problems that expand NASA capabilities in conducting space activities. It has been illustrated that the complexity of simulations of particle interaction can be reduced from an exponential one to a polynomial one.

This work was done by Michail Zak of Caltech for NASA's Jet Propulsion Laboratory. For more information, contact iaoffice@jpl.nasa.gov. NPO-47158

▶ Reconstituted Three-Dimensional Interactive Imaging

Lyndon B. Johnson Space Center, Houston, Texas

A method combines two-dimensional images, enhancing the images as well as rendering a 3D, enhanced, interactive computer image or visual model. Any advanced compiler can be used in conjunction with any graphics library package for this method, which is intended to take digitized images and virtually stack them so that they can be interactively viewed as a set of slices. This innovation can take multiple image sources (film or digital) and create a “transparent” image with higher densi-

ties in the image being less transparent. The images are then stacked such that an apparent 3D object is created in virtual space for interactive review of the set of images.

This innovation can be used with any application where 3D images are taken as slices of a larger object. These could include machines, materials for inspection, geological objects, or human scanning.

Illuminous values were stacked into planes with different transparency levels of tissues. These transparency levels can

use multiple energy levels, such as density of CT scans or radioactive density. A desktop computer with enough video memory to produce the image is capable of this work. The memory changes with the size and resolution of the desired images to be stacked and viewed.

This work was done by Joseph Hamilton, Theodore Foley, and Thomas Duncavage of Johnson Space Center and Terrence Mayes of Barrios Technology. For further information, contact the JSC Innovation Partnerships Office at (281) 483-3809. MSC-23860-1

▶ Determining Atmospheric-Density Profile of Titan

NASA's Jet Propulsion Laboratory, Pasadena, California

A method was developed for measuring the atmospheric density of Titan, the largest moon of Saturn, to create an accurate density profile as a function of altitude. This will allow mission planners to select safe flyby altitudes, and for navigation engineers to accurately predict the delta-v associated with those flybys.

The spacecraft angular rate vector profile as a function of time is collected via telemetry from the onboard attitude estimator once every 2 seconds. The telemetry for thruster times, as a func-

tion of time, for eight Reaction Control System (RCS) thrusters is gathered, once a second, from the Propulsion Manager algorithm of the Cassini onboard attitude-control flight software. Using these data, the ground software computes the angular momentum vector profile and the per-axis external torque as a function of time imparted from the spacecraft only due to the atmospheric drag. The software can then determine the Titan atmospheric density profile as a function of time and alti-

tude with the known values of spacecraft center of mass, the Titan-relative range and velocity data, the projected area, and the aerocenter, along with the estimated drag coefficient in a free molecular flow field.

This work was done by Siamak Sarani of Caltech for NASA's Jet Propulsion Laboratory.

The software used in this innovation is available for commercial licensing. Please contact Daniel Broderick of the California Institute of Technology at danielb@caltech.edu. Refer to NPO-44707.



Digital Microfluidics Sample Analyzer

Combined innovations enable portable analyzers for medical diagnostics, bioterrorism pathogen detection, and food supply analysis.

Lyndon B. Johnson Space Center, Houston, Texas

Three innovations address the needs of the medical world with regard to microfluidic manipulation and testing of physiological samples in ways that can benefit point-of-care needs for patients such as premature infants, for which drawing of blood for continuous tests can be life-threatening in their own right, and for expedited results. A chip with sample injection elements, reservoirs (and waste), droplet formation structures, fluidic pathways, mixing areas, and optical detection sites, was fabricated to test the various components of the microfluidic platform, both individually and in integrated fashion. The droplet control system permits a user to control droplet microactuator system functions, such as droplet operations and detector operations. Also, the programming system allows a user to develop software routines for controlling droplet microactuator system functions, such as droplet operations and detector operations.

A chip is incorporated into the system with a controller, a detector, input and output devices, and software. A novel filler fluid formulation is used for the transport of droplets with high protein concentrations. Novel assemblies for detection of photons from an on-chip droplet are present, as well as novel systems for conducting various assays, such as immunoassays and PCR (polymerase chain reaction).

The lab-on-a-chip (a.k.a., lab-on-a-printed-circuit board) processes physiological samples and comprises a system for automated, multi-analyte measurements using sub-microliter samples of human serum. The invention also relates to a diagnostic chip and system including the chip that performs many of the routine operations of a central lab-based chemistry analyzer, integrating, for example, colorimetric assays (e.g., for proteins), chemiluminescence/fluorescence assays (e.g., for enzymes, electrolytes, and gases), and/or conductometric assays (e.g., for hematocrit on plasma and whole blood) on a single chip platform.

Microfluidic control is essential for a successful lab-on-a-chip. This innovation is capable of analysis of bodily fluids such as blood, sweat, tears, serum, plasma, cerebrospinal fluid, sweat, and urine. It can be configured as a mobile or handheld instrument for use at bedside, ICU (intensive care unit), ER (emergency room), operating rooms, clinics, or in the field. Alternatively, it can be configured as a benchtop system. The chip can be configured to perform on-chip all-electrical micropumping; i.e., the chip can be configured to operate with no off-chip pressure sources or syringe pumps. Additionally, it can perform many simultaneous, parallel operations on nanodroplets, thereby expediting production of results.

To aid in processing the microfluidic samples, an improved design for loading a droplet actuator includes a top substrate that combines glass with one or more other materials that are easier to manufacture. Examples of such materials include resins and plastics. The glass-plate portion covers the droplet operations area of the droplet actuator, providing a flat, smooth surface for facilitating effective droplet operations. The plastic portion has one or more openings that provide a fluid path, from an exterior well, into the gap of the droplet actuator. The substrates are associated with electrodes for conducting droplet operations such as droplet transport and droplet dispensing.

This work was done by Michael G. Pollack, Vijay Srinivasan, Allen Eckhardt, Philip Y. Paik, Arjun Sudarsan, Alex Shenderov, Zhis-han Hua, and Vamsee K. Pamula of Advanced Liquid Logic, Inc. for Johnson Space Center. For further information, contact the JSC Innovation Partnerships Office at (281) 483-3809.

In accordance with Public Law 96-517, the contractor has elected to retain title to this invention. Inquiries concerning rights for its commercial use should be addressed to:

Advanced Liquid Logic Inc.

615 Davis Drive

Suite 800

P.O. Box 14025

Research Triangle Park, NC 27709

Refer to MSC-24283-1/553-1/4-1, volume and number of this Medical Design Briefs issue, and the page number.

Radiation Protection Using Carbon Nanotube Derivatives

This technology can be used in clinical oncology and in nuclear disaster response.

Lyndon B. Johnson Space Center, Houston, Texas

BHA and BHT are well-known food preservatives that are excellent radical scavengers. These compounds, attached to single-walled carbon nanotubes (SWNTs), could serve as excellent radical traps. The amino-BHT groups can be associated with SWNTs that have car-

bolyx acid groups via acid-base association or via covalent association.

The material can be used as a means of radiation protection or cellular stress mitigation via a sequence of quenching radical species using nano-engineered scaffolds of SWNTs and their deriva-

tives. It works by reducing the number of free radicals within or nearby a cell, tissue, organ, or living organism. This reduces the risk of damage to DNA and other cellular components that can lead to chronic and/or acute pathologies, including (but not limited to) can-

cer, cardiovascular disease, immunosuppression, and disorders of the central nervous system. These derivatives can show an unusually high scavenging ability, which could prove efficacious in protecting living systems from radical-induced decay.

This technique could be used to protect healthy cells in a living biological system from the effects of radiation therapy. It could also be used as a prophylactic or antidote for radiation exposure due to accidental, terrorist, or wartime use of radiation-containing weapons; high-altitude or space travel (where radiation ex-

posure is generally higher than desired); or in any scenario where exposure to radiation is expected or anticipated.

This invention's ultimate use will be dependent on the utility in an overall biological system where many levels of toxicity have to be evaluated. This can only be assessed at a later stage. *In vitro* toxicity will first be assessed, followed by *in vivo* non-mammalian screening in zebra fish for toxicity and therapeutic efficacy.

This work was done by Jodie L. Conyers, Jr., Valerie C. Moore, and S. Ward Casscells of the University of Texas Health Science Center at Houston for Johnson Space Center. For fur-

ther information, contact the JSC Innovation Partnerships Office at (281) 483-3809.

In accordance with Public Law 96-517, the contractor has elected to retain title to this invention. Inquiries concerning rights for its commercial use should be addressed to:

The University of Texas

*The Office of Technology Management
UCT 720,*

Houston, TX 77030

Phone No.: (713) 500-3369

E-mail: uthsch-otm@uth.tmc.edu

Refer to MSC-24565-1, volume and number of this NASA Tech Briefs issue, and the page number.

Process to Selectively Distinguish Viable From Non-Viable Bacterial Cells

NASA's Jet Propulsion Laboratory, Pasadena, California

The combination of ethidium monoazide (EMA) and post-fragmentation, randomly primed DNA amplification technologies will enhance the analytical capability to discern viable from non-viable bacterial cells in spacecraft-related samples. Intercalating agents have been widely used since the inception of molecular biology to stain and visualize nucleic acids. Only recently, intercalating agents such as EMA have been exploited to selectively distinguish viable from dead bacterial cells.

Intercalating dyes can only penetrate the membranes of dead cells. Once through the membrane and actually inside the cell, they intercalate DNA and, upon photolysis with visible light, produce stable DNA monoadducts. Once the DNA is crosslinked, it becomes insoluble and unable to be fragmented for post-fragmentation, randomly primed DNA library formation. Viable organisms' DNA remains unaffected by the intercalating agents, allowing for

amplification via post-fragmentation, randomly primed technologies. This results in the ability to carry out downstream nucleic acid-based analyses on viable microbes to the exclusion of all non-viable cells.

This work was done by Myron T. La Duc, James N. Benardini, and Christina N. Stam of Caltech for NASA's Jet Propulsion Laboratory. For more information, contact iaoffice@jpl.nasa.gov. NPO-47218



▶ **TEAMS Model Analyzer**

NASA's Jet Propulsion Laboratory, Pasadena, California

The TEAMS model analyzer is a supporting tool developed to work with models created with TEAMS (Testability, Engineering, and Maintenance System), which was developed by QSI.

In an effort to reduce the time spent in the manual process that each TEAMS modeler must perform in the preparation of reporting for model reviews, a new tool has been developed as an aid to models developed in TEAMS. The software allows for the viewing, reporting, and checking of TEAMS models that are checked into

the TEAMS model database. The software allows the user to selectively model in a hierarchical tree outline view that displays the components, failure modes, and ports. The reporting features allow the user to quickly gather statistics about the model, and generate an input/output report pertaining to all of the components. Rules can be automatically validated against the model, with a report generated containing resulting inconsistencies.

In addition to reducing manual effort, this software also provides an automated

process framework for the Verification and Validation (V&V) effort that will follow development of these models. The aid of such an automated tool would have a significant impact on the V&V process.

This work was done by Raffi P. Tikidjian of Caltech for NASA's Jet Propulsion Laboratory. Further information is contained in a TSP (see page 1).

This software is available for commercial licensing. Please contact Daniel Broderick of the California Institute of Technology at danielb@caltech.edu. Refer to NPO-46842.

▶ **Probabilistic Design and Analysis Framework**

John H. Glenn Research Center, Cleveland, Ohio

PRODAF is a software package designed to aid analysts and designers in conducting probabilistic analysis of components and systems. PRODAF can integrate multiple analysis programs to ease the tedious process of conducting a complex analysis process that requires the use of multiple software packages. The work uses a commercial finite element analysis (FEA) program with modules from NESSUS to conduct a probabilistic analysis of a hypothetical turbine blade, disk, and shaft model. PRODAF applies the response surface method, at the component level, and extrapolates the component-level responses to the system level. Hypothetical components

of a gas turbine engine are first deterministically modeled using FEA. Variations in selected geometrical dimensions and loading conditions are analyzed to determine the effects of the stress state within each component.

Geometric variations include the cord length and height for the blade, inner radius, outer radius, and thickness, which are varied for the disk. Probabilistic analysis is carried out using developing software packages like System Uncertainty Analysis (SUA) and PRODAF. PRODAF was used with a commercial deterministic FEA program in conjunction with modules from the probabilistic analysis program, NESTEM, to perturb

loads and geometries to provide a reliability and sensitivity analysis. PRODAF simplified the handling of data among the various programs involved, and will work with many commercial and open-source deterministic programs, probabilistic programs, or modules.

This work was done by William C. Strack and Vinod K. Nagpal of N&R Engineering for Glenn Research Center. Further information is contained in a TSP (see page 1).

Inquiries concerning rights for the commercial use of this invention should be addressed to NASA Glenn Research Center, Innovative Partnerships Office, Attn: Steve Fedor, Mail Stop 4-8, 21000 Brookpark Road, Cleveland, Ohio 44135. Refer to LEW-18372-1.

⚙ **Excavator Design Validation**

John H. Glenn Research Center, Cleveland, Ohio

The Excavator Design Validation tool verifies excavator designs by automatically generating control systems and modeling their performance in an accurate simulation of their expected environment. Part of this software design includes interfacing with human operations that can be included in simulation-based studies and validation. This is essential for assessing productivity, versatility, and reliability.

This software combines automatic control system generation from CAD (computer-aided design) models, rapid validation of complex mechanism designs, and detailed models of the environment including soil, dust, temperature, remote supervision, and communication latency to create a system of high value. Unique algorithms have been created for controlling and simulating complex robotic

mechanisms automatically from just a CAD description. These algorithms are implemented as a commercial cross-platform C++ software toolkit that is configurable using the Extensible Markup Language (XML).

The algorithms work with virtually any mobile robotic mechanisms using module descriptions that adhere to the XML standard. In addition, high-fidelity, real-

time physics-based simulation algorithms have also been developed that include models of internal forces and the forces produced when a mechanism interacts with the outside world. This capability is combined with an innovative organization for simulation algorithms, new regolith simulation methods, and a unique control and study architecture to make powerful tools with the potential to transform the way NASA verifies and compares excavator designs.

Energid's Actin software has been leveraged for this design validation. The architecture includes parametric and Monte Carlo studies tailored for

validation of excavator designs and their control by remote human operators. It also includes the ability to interface with third-party software and human-input devices. Two types of simulation models have been adapted: high-fidelity discrete element models and fast analytical models. By using the first to establish parameters for the second, a system has been created that can be executed in real time, or faster than real time, on a desktop PC. This allows Monte Carlo simulations to be performed on a computer platform available to all researchers, and it allows human interaction to be included in a

real-time simulation process. Metrics on excavator performance are established that work with the simulation architecture. Both static and dynamic metrics are included.

This work was done by Chalongrath Pholsiri, James English, Charles Seberino, and Yi-Je Lim of Energid Technologies for Glenn Research Center. Further information is contained in a TSP (see page 1).

Inquiries concerning rights for the commercial use of this invention should be addressed to NASA Glenn Research Center, Innovative Partnerships Office, Attn: Steve Fedor, Mail Stop 4-8, 21000 Brookpark Road, Cleveland, Ohio 44135. Refer to LEW-18522-1.

Observing System Simulation Experiment (OSSE) for the HypsIRI Spectrometer Mission

NASA's Jet Propulsion Laboratory, Pasadena, California

The OSSE software provides an integrated end-to-end environment to simulate an Earth observing system by iteratively running a distributed modeling workflow based on the HypsIRI Mission, including atmospheric radiative transfer, surface albedo effects, detection, and retrieval for agile exploration of the mission design space.

The software enables an Observing System Simulation Experiment (OSSE) and can be used for design trade space exploration of science return for proposed instruments by modeling the whole ground truth, sensing, and retrieval chain and to assess retrieval accuracy for a particular instrument and algorithm design. The OSSE infrastructure is extensible to future National Research Council (NRC) Decadal Survey concept missions where integrated modeling can improve the fidelity of coupled science and engineering analyses for systematic analysis and

science return studies.

This software has a distributed architecture that gives it a distinct advantage over other similar efforts. The workflow modeling components are typically legacy computer programs implemented in a variety of programming languages, including MATLAB, Excel, and FORTRAN. Integration of these diverse components is difficult and time-consuming. In order to hide this complexity, each modeling component is wrapped as a Web Service, and each component is able to pass analysis parameterizations, such as reflectance or radiance spectra, on to the next component downstream in the service workflow chain. In this way, the interface to each modeling component becomes uniform and the entire end-to-end workflow can be run using any existing or custom workflow processing engine. The architecture lets users extend workflows as new modeling components become available, chain to-

gether the components using any existing or custom workflow processing engine, and distribute them across any Internet-accessible Web Service endpoints.

The workflow components can be hosted on any Internet-accessible machine. This has the advantages that the computations can be distributed to make best use of the available computing resources, and each workflow component can be hosted and maintained by their respective domain experts.

This work was done by Michael J. Turmon, Gary L. Block, Robert O. Green, Hook Hua, Joseph C. Jacob, Harold R. Sobel, and Paul L. Springer of Caltech and Qingyuan Zhang of the University of Maryland, Baltimore County (UMBC) for NASA's Jet Propulsion Laboratory. Further information is contained in a TSP (see page 1).

This software is available for commercial licensing. Please contact Daniel Broderick of the California Institute of Technology at danielb@caltech.edu. Refer to NPO-47048.

Momentum Management Tool for Low-Thrust Missions

NASA's Jet Propulsion Laboratory, Pasadena, California

A momentum management tool was designed for the Dawn low-thrust interplanetary spacecraft en route to the asteroids Vesta and Ceres, in an effort to better understand the early creation of the solar system. Momentum must be managed to ensure the spacecraft has

enough control authority to perform necessary turns and hold a fixed inertial attitude against external torques. Along with torques from solar pressure and gravity-gradients, ion-propulsion engines produce a torque about the thrust axis that must be countered by

the four reaction wheel assemblies (RWA).

MomProf is a ground operations tool built to address these concerns. The momentum management tool was developed during initial checkout and early cruise, and has been refined to accommodate a

wide range of momentum-management issues. With every activity or sequence, wheel speeds and momentum state must be checked to avoid undesirable conditions and use of consumables.

MomProf was developed to operate in the MATLAB environment. All data are loaded into MATLAB as a structure to provide consistent access to all inputs by individual functions within the tool. Used in its most basic application,

the Dawn momentum tool uses the basic principle of angular momentum conservation, computing momentum in the body frame, and RWA wheel speeds, for all given orientations in the input file.

MomProf was designed specifically to be able to handle the changing external torques and frequent desaturations. Incorporating significant external torques adds complexity

since there are various external torques that act under different operational modes.

This work was done by Edward R. Swenka, Brett A. Smith, and Charles A. Vanelli of Caltech for NASA's Jet Propulsion Laboratory.

This software is available for commercial licensing. Please contact Daniel Broderick of the California Institute of Technology at danielb@caltech.edu. Refer to NPO-46435.

Mixed Real/Virtual Operator Interface for ATHLETE

NASA's Jet Propulsion Laboratory, Pasadena, California

The mixed real/virtual operator interface for ATHLETE (MSim-ATHLETE) is a new software system for operating manipulation and inspection tasks in JPL's ATHLETE (All-Terrain Hex-Legged Extra-Terrestrial Explorer). The system presents the operator with a graphical model of the robot and a palette of available joint types. Once virtual articulations are constructed for a task, the operator can move any joint or link, and the system interactively responds in real-time with a compatible motion for all joints that best satisfies all constraints.

Unique features of the software include:

- On-line topological dynamism: The key feature of MSim-ATHLETE is that it permits the kinematic structure of

the operated mechanism to be changed dynamically by the operator. These changes are not (usually) meant to indicate actual changes in the physical system, but rather add/remove virtual extensions for constraining and parameterizing motions.

- Mixed reification: MSim-ATHLETE models two kinds of articulations: real articulations model the robot and virtual articulations model the virtual extensions.
- Pure kinematicity: MSim-ATHLETE is purely kinematic and thus does not require specifying any physics parameters, such as mass and friction properties.
- Useful handling of under- and over-constraint: MSim-ATHLETE allows

the operator to specify both under- and over-constrained motions. In both cases, several features help organize and structure the result, including prioritized constraints, explicit hierarchical decomposition, and least-squares solving.

This work was done by Jeffrey S. Norris and David S. Mittman of Caltech and Marsette A. Vona and Daniela Rus of Massachusetts Institute of Technology for NASA's Jet Propulsion Laboratory. For more information, see <http://www.mit.edu/~vona/MSim-ATHLETE/MSim-ATHLETE-info.html>.

This software is available for commercial licensing. Please contact Daniel Broderick of the California Institute of Technology at danielb@caltech.edu. Refer to NPO-46869.

Antenna Controller Replacement Software

NASA's Jet Propulsion Laboratory, Pasadena, California

The Antenna Controller Replacement (ACR) software accurately points and monitors the Deep Space Network (DSN) 70-m and 34-m high-efficiency (HEF) ground-based antennas that are used to track primarily spacecraft and, periodically, celestial targets. To track a spacecraft, or other targets, the antenna must be accurately pointed at the spacecraft, which can be very far away with very weak signals. ACR's conical scanning capability collects the signal in a circular pattern around the target, calculates the location of the strongest signal, and adjusts the antenna pointing to point directly at the spacecraft. A real-time, closed-loop servo control algorithm performed every 0.02 second allows accurate positioning of the antenna in order to track these distant

spacecraft. Additionally, this advanced servo control algorithm provides better antenna pointing performance in windy conditions.

The ACR software provides high-level commands that provide a very easy user interface for the DSN operator. The operator only needs to enter two commands to start the antenna and subreflector, and Master Equatorial tracking. The most accurate antenna pointing is accomplished by aligning the antenna to the Master Equatorial, which because of its small size and sheltered location, has the most stable pointing. The antenna has hundreds of digital and analog monitor points. The ACR software provides compact displays to summarize the status of the antenna, subreflector, and

the Master Equatorial.

The ACR software has two major functions. First, it performs all of the steps required to accurately point the antenna (and subreflector and Master Equatorial) at the spacecraft (or celestial target). This involves controlling the antenna/subreflector/Master-Equatorial hardware, initiating and monitoring the correct sequence of operations, calculating the position of the spacecraft relative to the antenna, executing the real-time servo control algorithm to maintain the correct position, and monitoring tracking performance.

Second, the ACR software monitors the status and performance of the antenna, subreflector, and Master Equatorial for the safety of personnel and of the antenna equipment. While track-

ing occurs during scheduled periods every day of the week, the ACR software continuously monitors the antenna equipment.

This work was done by Roger Y. Chao, Scott C. Morgan, Martha M. Strain,

Stephen T. Rockwell, Kenneth J. Shimizu, Barzia J. Tehrani, Jaclyn H. Kwok, Michelle Tuazon-Wong, and Henry Valtier of Caltech; Reza Nalbandi of MTC; Michael Wert of ITT; and Patrick Leung of ISDS/Averstar for NASA's Jet Propulsion

Laboratory. For more information, contact iaoffice@jpl.nasa.gov.

This software is available for commercial licensing. Please contact Daniel Broderick of the California Institute of Technology at danielb@caltech.edu. Refer to NPO-47002.

Efficient Parallel Engineering Computing on Linux Workstations

NASA's Jet Propulsion Laboratory, Pasadena, California

A C software module has been developed that creates lightweight processes (LWPs) dynamically to achieve parallel computing performance in a variety of engineering simulation and analysis applications to support NASA and DoD project tasks. The required interface between the module and the application it supports is simple, minimal and almost completely transparent to the user applications, and it can achieve nearly ideal computing speed-up on multi-CPU engineering workstations of all operating system platforms. The module can be integrated into an existing application (C, C++, Fortran and others) either as part of a compiled module or as a dynamically linked library (DLL).

This software has the following major advantages over existing commercial and public domain software of similar functionality.

1. It is especially applicable to and powerful on commercially, widely available, multi-CPU engineering workstations;
2. It has a very simple software architecture and user interface and can be quickly integrated into an existing application; and
3. Its code size is very small, and its performance overhead is minimal, resulting in nearly ideal parallel-computing performance for many computing-intensive scientific and engineering applications.

The approach adopted in this technology development does not require any additional hardware and software beyond what's typically available on any commercial engineering workstations, that is a native operating system and C, C++ or FORTRAN compilers that an application needs.

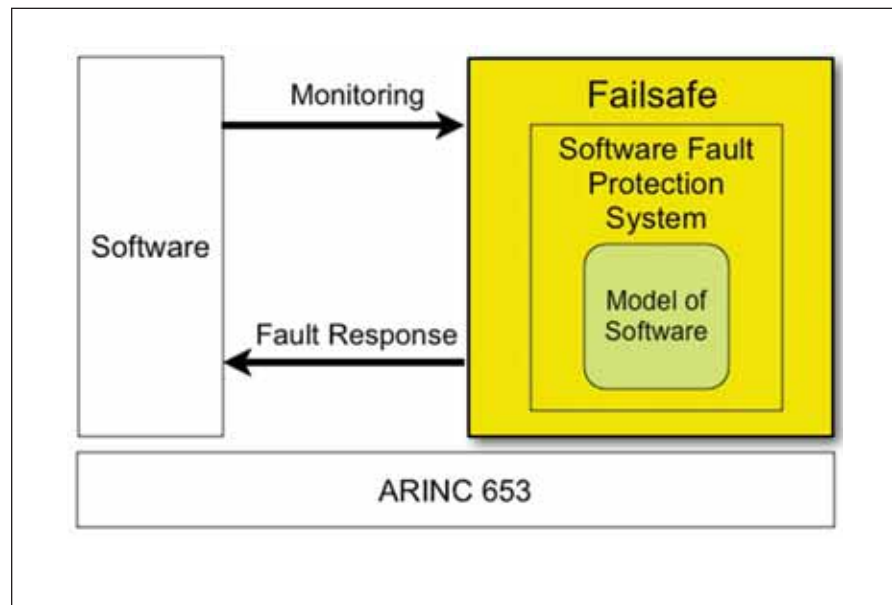
This work was done by John Z. Lou of Caltech for NASA's Jet Propulsion Laboratory. For more information, contact iaoffice@jpl.nasa.gov.

The software used in this innovation is available for commercial licensing. Please contact Daniel Broderick of the California Institute of Technology at danielb@caltech.edu. Refer to NPO-46892.

FAILSAFE Health Management for Embedded Systems

NASA's Jet Propulsion Laboratory, Pasadena, California

The FAILSAFE project is developing concepts and prototype implementations for software health management in mission-critical, real-time embedded systems. The project unites features of the industry-standard ARINC 653 Avionics Application Software Standard Interface and JPL's Mission Data System (MDS) technology (see figure). The ARINC 653 standard establishes requirements for the services provided by partitioned, real-time operating systems. The MDS technology provides a state analysis method, canonical architecture, and software framework that facilitates the design and implementation of software-intensive complex systems. The MDS technology has been used to provide the health management function for an ARINC 653 application implementation. In particular, the focus is on showing how this combination enables reasoning about, and recovering from, application software problems.



The FAILSAFE model-based health management concept is depicted in the block diagram.

The application itself consists of two unique applications running in the ARINC 653 system: a target application and the FAILSAFE model-based health monitoring application. The target application is a high-level simulation of the Shuttle Abort Control System (ACS), developed specifically for this task. The target application is a two-partition application with one partition allocated to the sequencing behavior, and one partition allocated to the application I/O. The health monitor application executes in its own partition. The three application partitions communicate via ARINC 653 ports and message queues, which are specified in the system module.xml configuration file. Real-time system data is provided to the health monitor via the use of ARINC 653 sampling ports that al-

lows the health monitor application to intercept any traffic coming across the ports of interest.

This task was turned into a goal-based function that, when working in concert with the software health manager, aims to work around software and hardware problems in order to maximize abort performance results. In order to make it a compelling demonstration for current aerospace initiatives, the prototype has been additionally imposed on a number of requirements derived from NASA's Constellation Program.

Lastly, the ARINC 653 standard imposes a number of requirements on the system integrator for developing the requisite error handler process. Under ARINC 653, the health monitoring (HM) service is invoked by an applica-

tion calling the application error service, or by the operating system or hardware detecting a fault. It is these HM and error process details that are implemented with the MDS technology, showing how a static-analytic approach is appropriate for identifying fault determination details, and showing how the framework supports acting upon state estimation and control features in order to achieve safety-related goals.

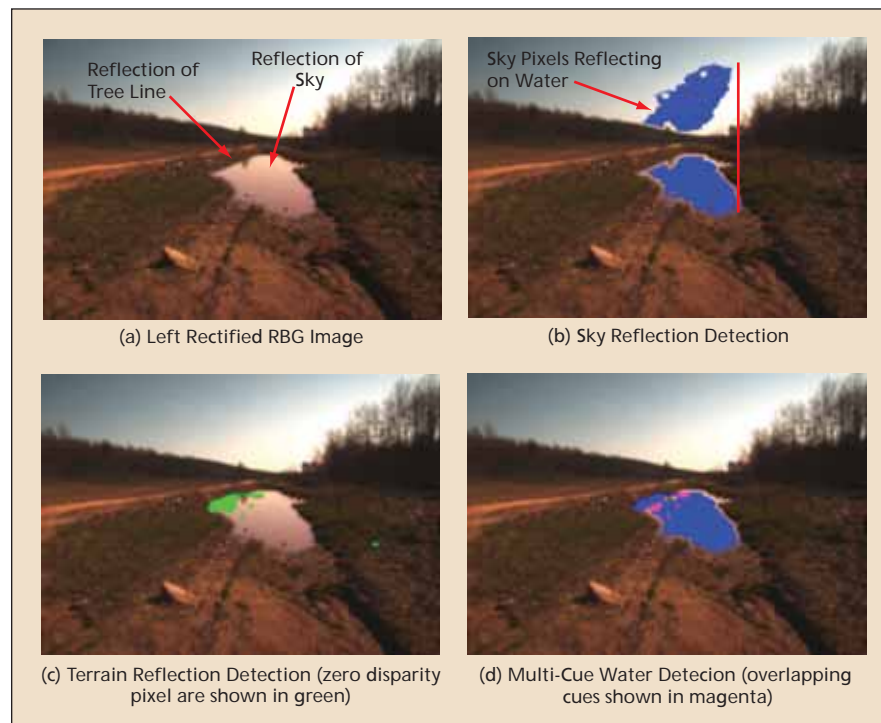
This work was done by Gregory A. Horvath, David A. Wagner, and Hui Ying Wen of Caltech and Matthew Barry of Kestrel Technology for NASA's Jet Propulsion Laboratory. For more information, contact iaoffice@jpl.nasa.gov.

This software is available for commercial licensing. Please contact Daniel Broderick of the California Institute of Technology at danielb@caltech.edu. Refer to NPO-46981.

Water Detection Based on Sky Reflections

NASA's Jet Propulsion Laboratory, Pasadena, California

This software has been designed to detect water bodies that are out in the open on cross-country terrain at mid- to far-range (approximately 20–100 meters), using imagery acquired from a stereo pair of color cameras mounted on a terrestrial, unmanned ground vehicle (UGV). Non-traversable water bodies, such as large puddles, ponds, and lakes, are indirectly detected by detecting reflections of the sky below the horizon in color imagery. The appearance of water bodies in color imagery largely depends on the ratio of light reflected off the water surface to the light coming out of the water body. When a water body is far away, the angle of incidence is large, and the light reflected off the water surface dominates. We have exploited this behavior to detect water bodies out in the open at mid- to far-range. When a water body is detected at far range, a UGV's path planner can begin to look for alternate routes to the goal position sooner, rather than later. As a result, detecting water hazards at far range generally reduces the time required to reach a goal position during autonomous navigation. This software implements a new water detector based on sky reflections that geometrically locates the exact pixel in the sky that is reflecting on a candidate water pixel on the ground, and predicts if the ground pixel is water based on color similarity and local terrain features (see figure).



Water is Detected indirectly by detecting sky and terrain reflections.

Assuming a water body can be modeled as a horizontal mirror, a ray of incident light reflected off the surface of a water body enters a pixel of a camera's focal plane array (FPA). Since the angle of incidence is equal to the angle of reflection (according to the law of reflection), a direct ray from the tail of the incident ray (and within the same

vertical plane as the incident ray) will enter the camera's FPA at a pixel whose color will indicate the color of the sky being reflected along the reflected ray. Because the distance between the camera and the sky is much larger than the distance between the camera and candidate water points at normal detection ranges, the direct ray and the incident

ray will be nearly parallel, and the angle between the direct ray and the reflected ray can be approximated as two times the glancing angle. Calculations to locate the pixel a direct ray enters are simple and involve for any candidate water pixel conversion of the 2D

image coordinates to a 3D unit vector, negation of the z component of the unit vector, and conversion of the modified unit vector back to 2D image coordinates.

This work was done by Arturo L. Rankin and Larry H. Matthies of Caltech for

NASA's Jet Propulsion Laboratory. Further information is contained in a TSP (see page 1).

This software is available for commercial licensing. Please contact Daniel Broderick of the California Institute of Technology at danielb@caltech.edu. Refer to NPO-47092.

Nonlinear Combustion Instability Prediction

Marshall Space Flight Center, Alabama

The liquid rocket engine stability prediction software (LCI) predicts combustion stability of systems using LOX-LH₂ propellants. Both longitudinal and transverse mode stability characteristics are calculated. This software has the unique feature of being able to predict system limit amplitude.

New methods for predicting stability have been created based on a detailed

physical understanding of the combustion instability problem, which has resulted in a computationally predictive algorithm that allows determination of pressure oscillation frequencies and geometry, growth rates for component modes of oscillation, development of steepened wave structures, limit (maximum) amplitude of oscillations, and changes in mean operation chamber conditions.

The program accommodates any combustion-chamber shape. The program can run on desktop computer systems, and is readily upgradeable as new data become available.

This program was written by Gary Flandro of the University of Tennessee, Space Institute, Calspan Center, for Marshall Space Flight Center. For further information, contact Sammy Nabors, MSFC Commercialization Assistance Lead, at sammy.a.nabors@nasa.gov. Refer to MFS-32549-1.

JMISR Interactive eXplorer

NASA's Jet Propulsion Laboratory, Pasadena, California

MISR (Multi-angle Imaging Spectroradiometer) Interactive eXplorer (MINX) is an interactive visualization program that allows a user to digitize smoke, dust, or volcanic plumes in MISR multiangle images, and automatically retrieve height and wind profiles associated with those plumes. This innovation can perform 9-camera animations of MISR level-1 radiance images to study the 3D relationships of clouds and plumes. MINX also enables archiving MISR aerosol properties and Moderate Resolution Imaging Spectroradiometer (MODIS) fire radiative power along with the heights and winds. It can correct geometric misregistration between cameras by correlating off-nadir camera scenes with corresponding nadir scenes and

then warping the images to minimize the misregistration offsets. Plots of BRF (bidirectional reflectance factor) vs. camera angle for points clicked in an image can be displayed. Users get rapid access to map views of MISR path and orbit locations and overflight dates, and past or future orbits can be identified that pass over a specified location at a specified time. Single-camera, level-1 radiance data at 1,100- or 275-meter resolution can be quickly displayed in color using a browse option.

This software determines the heights and motion vectors of features above the terrain with greater precision and coverage than previous methods, based on an algorithm that takes wind direction into consideration. Human interpreters can precisely identify plumes

and their extent, and wind direction. Overposting of MODIS thermal anomaly data aids in the identification of smoke plumes. The software has been used to preserve graphical and textural versions of the digitized data in a Web-based database that currently contains more than 7,000 smoke plumes (<http://www-misr2.jpl.nasa.gov/EPA-Plumes/>).

This work was done by David L. Nelson of Columbus Technologies and Services; David J. Diner; Charles K. Thompson, Jeffrey R. Hall, and Brian E. Rheingans of Caltech; Michael J. Garay of Raytheon; and Dominic Mazzoni of Google, Inc. for NASA's Jet Propulsion Laboratory. For more information, download the MINX software package and User's Guide at <http://www.openchannelsoftware.com/projects/MINX/>. NPO-47098

Characterization of Cloud Water-Content Distribution

NASA's Jet Propulsion Laboratory, Pasadena, California

The development of realistic cloud parameterizations for climate models requires accurate characterizations of sub-grid distributions of thermodynamic

variables. To this end, a software tool was developed to characterize cloud water-content distributions in climate-model sub-grid scales.

This software characterizes distributions of cloud water content with respect to cloud phase, cloud type, precipitation occurrence, and geo-location

using CloudSat radar measurements. It uses a statistical method called maximum likelihood estimation to estimate the probability density function of the cloud water content.

A crude treatment of sub-grid scale cloud processes in current climate models is widely recognized as a major limitation in predictions of global climate change. At present, typical climate models have a horizontal resolution on the order of 100

km and a variable vertical resolution between 100 m and 1 km. Since climate models cannot explicitly resolve what happens at the sub-grid scales, the physics must be parameterized as a function of the resolved motions. The fundamental problem of cloud parameterization is to characterize the distributions of cloud variables at sub-grid scales and to relate the sub-grid variations to the resolved flow. This software solves the problem by

estimating the probability density function of cloud water content at the sub-grid scale using CloudSat measurements.

This work was done by Seungwon Lee of Caltech for NASA's Jet Propulsion Laboratory. For more information, contact iaoffice@jpl.nasa.gov.

This software is available for commercial licensing. Please contact Daniel Broderick of the California Institute of Technology at danielb@caltech.edu. Refer to NPO-47248.

Autonomous Planning and Replanning for Mine-Sweeping Unmanned Underwater Vehicles

NASA's Jet Propulsion Laboratory, Pasadena, California

This software generates high-quality plans for carrying out mine-sweeping activities under resource constraints. The autonomous planning and replanning system for unmanned underwater vehicles (UUVs) takes as input a set of prioritized mine-sweep regions, and a specification of available UUV resources including available battery energy, data storage, and time available for accomplishing the mission. Mine-sweep areas vary in location, size of area to be swept, and importance of the region. The planner also works with a model of the UUV, as well as a model of the power con-

sumption of the vehicle when idle and when moving.

The planner begins by using a depth-first, branch-and-bound search algorithm to find an optimal mine sweep to maximize the value of the mine-sweep regions included in the plan, subjected to available resources. The software issues task commands to an underlying control architecture to carry out the activities on the vehicle, and to receive updates on the state of the world and the vehicle. During plan execution, the planner uses updates from the control system to make updates to the predic-

tions of the vehicle and world states. The effects of these updates are propagated into the future and allow the planner to detect conflicts ahead of time, or to identify any resource surplus that might exist and could allow the planner to include additional mine-sweep regions.

This work was done by Daniel M. Gaines of Caltech for NASA's Jet Propulsion Laboratory. For more information, contact iaoffice@jpl.nasa.gov.

This software is available for commercial licensing. Please contact Daniel Broderick of the California Institute of Technology at danielb@caltech.edu. Refer to NPO-47018.

Dayside Ionospheric Superfountain

NASA's Jet Propulsion Laboratory, Pasadena, California

The Dayside Ionospheric Superfountain modified SAMI2 code predicts the uplift, given storm-time electric fields, of the dayside near-equatorial ionosphere to heights of over 800 kilometers during magnetic storm intervals. This software is a simple 2D code devel-

oped over many years at the Naval Research Laboratory, and has importance relating to accuracy of GPS positioning, and for satellite drag.

This work was done by Bruce T. Tsurutani, Olga P. Verkhoglyadova, and Anthony J. Mannucci of Caltech for NASA's Jet Propul-

sion Laboratory. For more information, contact iaoffice@jpl.nasa.gov.

This software is available for commercial licensing. Please contact Daniel Broderick of the California Institute of Technology at danielb@caltech.edu. Refer to NPO-47209.

In-Situ Pointing Correction and Rover Microlocalization

NASA's Jet Propulsion Laboratory, Pasadena, California

Two software programs, *marstie* and *marsnav*, work together to generate pointing corrections and rover micro-localization for *in-situ* images. The programs are based on the PIG (Planetary Image Geometry) library, which handles all mission dependencies. As a result, there is no mis-

sion-specific code in either of these programs. This software corrects geometric seams in images as much as possible (some parallax seams are uncorrectable).

First, *marstie* is used to gather tie-points. The program analyzes the input image set, determines which images

overlap, and presents overlapping pairs to the user. The user then manually creates a number of tiepoints between each pair, by identifying the locations of features that are common to both images. An automatic correlator assists the user in getting subpixel accuracy on these tie-

points. Tiepoints may also be edited.

The tiepoints are then used by the second program, marsnav, to generate pointing corrections. This works by projecting one half of each tiepoint to a surface model and back into the other image. This projected location is then compared to the measured tiepoint and a residual error is determined. A global minimization process adjusts the pointing of each input frame until the optimal pointing is determined. The pointing is typically constrained to match possible physical camera motions, although the pointing model is selectable via the PIG library. The resulting “nav solution” is then input into the mosaic pro-

grams, which apply the pointing adjustment in order to make seamless mosaics.

In addition to adjusting the pointing, marsnav can also adjust the surface model (helpful when dealing with an unknown terrain), and the position and/or orientation of the rover itself. The latter results in a “micro-localization” — determining where the rover is and how it is oriented on a very fine scale.

Commercial mosaic-stitching programs exist. However, they typically perform unconstrained warping of the images in order to achieve a match. This results in an unknown geometry and unacceptable distortion. By correcting the

seams using this pointing-correction method, the result is constrained to be physically meaningful, and is accurate enough to be acceptable for use by science and ops teams. This method does, however, require *a priori* camera calibration information. The techniques are not limited to mast-mounted cameras; they have been successfully applied to arm cameras as well.

This work was done by Robert G. Deen and Jean J. Lorre of Caltech for NASA's Jet Propulsion Laboratory.

This software is available for commercial licensing. Please contact Daniel Broderick of the California Institute of Technology at danielb@caltech.edu. Refer to NPO-46696.

Operation Program for the Spatially Phase-Shifted Digital Speckle Pattern Interferometer — SPS-DSPI

Goddard Space Flight Center, Greenbelt, Maryland

SPS-DSPI software has been revised so that Goddard optical engineers can operate the instrument, instead of data programmers. The user interface has been improved to view the data collected by the SPS-DSPI, with a real-time mode and a play-back mode. The SPS-DSPI has been developed by NASA/GSFC to measure the temperature distortions of the primary-mirror backplane structure for the James Webb Space Telescope. It requires a

team of computer specialists to run successfully, because, at the time of this reporting, it just finished the prototype stage. This software improvement will transition the instrument to become available for use by many programs that measure distortion.

Dead code from earlier versions has been removed. The tighter code has been refactored to improve usability and maintainability. A prototype GUI has been created to run this refactored

code. A big improvement is the ability to test the monitors and real-time functions without running the laser, by using a data acquisition simulator.

This work was done by Peter N. Blake, Joycelyn T. Jones, and Carl E. Hostetter of Goddard Space Flight Center and Perry Greenfield and Todd Miller of AURA Space Telescope Science Institute. For further information, contact the Goddard Innovative Partnerships Office at (301) 286-5810. GSC-15709-1

GOATS - Orbitology Component

NASA's Jet Propulsion Laboratory, Pasadena, California

The GOATS Orbitology Component software was developed to specifically address the concerns presented by orbit analysis tools that are often written as stand-alone applications. These applications do not easily interface with standard JPL first-principles analysis tools, and have a steep learning curve due to their complicated nature. This toolset is written as a series of MATLAB functions, allowing seamless integration into existing JPL optical systems engineering modeling and analysis modules. The functions are completely open, and allow for advanced users to delve into and modify the underlying physics being modeled. Additionally, this software module fills an analysis gap, allowing for

quick, high-level mission analysis trades without the need for detailed and complicated orbit analysis using commercial stand-alone tools.

This software consists of a series of MATLAB functions to provide for geometric orbit-related analysis. This includes propagation of orbits to varying levels of generalization. In the simplest case, geosynchronous orbits can be modeled by specifying a subset of three orbit elements. The next case is a circular orbit, which can be specified by a subset of four orbit elements. The most general case is an arbitrary elliptical orbit specified by all six orbit elements. These orbits are all solved geometrically, under the basic

problem of an object in circular (or elliptical) orbit around a rotating spheroid. The orbit functions output time series ground tracks, which serve as the basis for more detailed orbit analysis. This software module also includes functions to track the positions of the Sun, Moon, and arbitrary celestial bodies specified by right ascension and declination. Also included are functions to calculate line-of-sight geometries to ground-based targets, angular rotations and decompositions, and other line-of-site calculations.

The toolset allows for the rapid execution of orbit trade studies at the level of detail required for the early stage of mission concept development.

Additionally, once orbit parameters are settled upon, the same tools can be used to model system performance, and execute more focused trade studies as requirements are being developed and analyzed. This toolset offers a cohesive

model-based systems engineering tool to be used as mission concepts are developed and in the development and analysis of top-level system requirements.

This work was done by Benjamin M. Haber and Joseph J. Green of Caltech for

NASA's Jet Propulsion Laboratory. For more information, contact iaoffice@jpl.nasa.gov.

This software is available for commercial licensing. Please contact Daniel Broderick of the California Institute of Technology at danielb@caltech.edu. Refer to NPO-47236.

Hybrid-PIC Computer Simulation of the Plasma and Erosion Processes in Hall Thrusters

NASA's Jet Propulsion Laboratory, Pasadena, California

HPHall software simulates and tracks the time-dependent evolution of the plasma and erosion processes in the discharge chamber and near-field plume of Hall thrusters. HPHall is an axisymmetric solver that employs a hybrid fluid/particle-in-cell (Hybrid-PIC) numerical approach. HPHall, originally developed by MIT in 1998, was upgraded to HPHall-2 by the Polytechnic University of Madrid in 2006. The Jet Propulsion Laboratory has continued the development of HPHall-2 through

upgrades to the physical models employed in the code, and the addition of entirely new ones.

Primary among these are the inclusion of a three-region electron mobility model that more accurately depicts the cross-field electron transport, and the development of an erosion sub-model that allows for the tracking of the erosion of the discharge chamber wall. The code is being developed to provide NASA science missions with a predictive tool of Hall thruster performance and

lifetime that can be used to validate Hall thrusters for missions.

This work was done by Richard R. Hofer, Ira Katz, and Ioannis G. Mikellides of Caltech and Manuel Gamero-Castano of the University of California, Irvine for NASA's Jet Propulsion Laboratory. Further information is contained in a TSP (see page 1).

This software is available for commercial licensing. Please contact Daniel Broderick of the California Institute of Technology at danielb@caltech.edu. Refer to NPO-46513.

BioNet Digital Communications Framework

John H. Glenn Research Center, Cleveland, Ohio

BioNet v2 is a peer-to-peer middleware that enables digital communication devices to "talk" to each other. It provides a software development framework, standardized application, network-transparent device integration services, a flexible messaging model, and network communications for distributed applications. BioNet is an implementation of the Constellation Program Command, Control, Communications and Information (C3I) Interoperability specification, given in CxP 70022-01.

The system architecture provides the necessary infrastructure for the integra-

tion of heterogeneous wired and wireless sensing and control devices into a unified data system with a standardized application interface, providing plug-and-play operation for hardware and software systems.

BioNet v2 features a naming schema for mobility and coarse-grained localization information, data normalization within a network-transparent device driver framework, enabling of network communications to non-IP devices, and fine-grained application control of data subscription bandwidth usage. BioNet directly integrates Disruption Tolerant Networking

(DTN) as a communications technology, enabling networked communications with assets that are only intermittently connected including orbiting relay satellites and planetary rover vehicles.

This work was done by Kevin Gifford, Sebastian Kuzminsky, and Shea Williams of the University of Colorado at Boulder for Glenn Research Center.

Inquiries concerning rights for the commercial use of this invention should be addressed to NASA Glenn Research Center, Innovative Partnerships Office, Attn: Steve Fedor, Mail Stop 4-8, 21000 Brookpark Road, Cleveland, Ohio 44135. Refer to LEW-18415-1

Real-Time Feature Tracking Using Homography

NASA's Jet Propulsion Laboratory, Pasadena, California

This software finds feature point correspondences in sequences of images. It is designed for feature matching in aerial imagery. Feature matching is a fundamental step in a number of important image processing operations: calibrating the cameras in a camera array, stabilizing im-

ages in aerial movies, geo-registration of images, and generating high-fidelity surface maps from aerial movies.

The method uses a Shi-Tomasi corner detector and normalized cross-correlation. This process is likely to result in the production of some mismatches. The

feature set is cleaned up using the assumption that there is a large planar patch visible in both images. At high altitude, this assumption is often reasonable. A mathematical transformation, called an homography, is developed that allows us to predict the position in

image 2 of any point on the plane in image 1. Any feature pair that is inconsistent with the homography is thrown out. The output of the process is a set of feature pairs, and the homography.

The algorithms in this innovation are well known, but the new implementation improves the process in several ways. It runs in real-time at 2 Hz on 64-megapixel imagery. The new Shi-Tomasi corner detector tries to produce the re-

quested number of features by automatically adjusting the minimum distance between found features. The homography-finding code now uses an implementation of the RANSAC algorithm that adjusts the number of iterations automatically to achieve a pre-set probability of missing a set of inliers. The new interface allows the caller to pass in a set of predetermined points in one of the images. This allows the ability to track the

same set of points through multipleframes.

This work was done by Daniel S. Clouse, Yang Cheng, Adnan I. Ansar, David C. Trotz, and Curtis W. Padgett of Caltech for NASA's Jet Propulsion Laboratory. Further information is contained in a TSP (see page 1).

The software used in this innovation is available for commercial licensing. Please contact Daniel Broderick of the California Institute of Technology at danielb@caltech.edu. Refer to NPO-46916.

▶ Sparse Superpixel Unmixing for Hyperspectral Image Analysis

NASA's Jet Propulsion Laboratory, Pasadena, California

Software was developed that automatically detects minerals that are present in each pixel of a hyperspectral image. An algorithm based on sparse spectral unmixing with Bayesian Positive Source Separation is used to produce mineral abundance maps from hyperspectral images. A "superpixel" segmentation strategy enables efficient unmixing in an interactive session.

The algorithm computes statistically likely combinations of constituents based on a set of possible constituent minerals whose abundances are uncertain. A library of source spectra from laboratory experiments or previous remote observations is used. A superpixel segmentation strategy improves analysis time by orders of magnitude, permitting incorporation into an interactive user session (see figure).

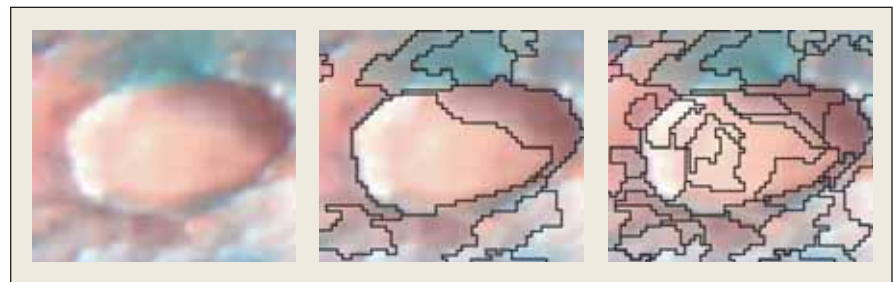
Mineralogical search strategies can be categorized as "supervised" or "unsupervised." Supervised methods use a detec-

tion function, developed on previous data by hand or statistical techniques, to identify one or more specific target signals. Purely unsupervised results are not always physically meaningful, and may ignore subtle or localized mineralogy since they aim to minimize reconstruction error over the entire image. This algorithm offers advantages of both methods, providing meaningful physical interpretations and sensitivity to subtle or unex-

pected minerals.

This work was done by Rebecca Castano and David R. Thompson of Caltech and Martha Gilmore of Wesleyan University for NASA's Jet Propulsion Laboratory. For more information, contact iaoffice@jpl.nasa.gov.

The software used in this innovation is available for commercial licensing. Please contact Daniel Broderick of the California Institute of Technology at danielb@caltech.edu. Refer to NPO-47038.



Here a Subwindow of Observation demonstrates superpixel segmentation. Left: original subimage. Center: coarse segmentation, minimum region size 100. Right: fine segmentation, minimum region size 20.

▶ Intelligent Patching of Conceptual Geometry for CFD Analysis

Langley Research Center, Hampton, Virginia

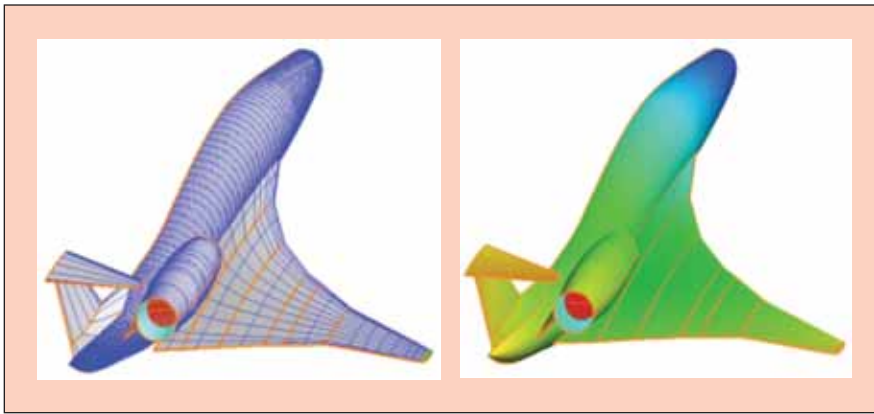
The iPatch computer code for intelligently patching surface grids was developed to convert conceptual geometry to computational fluid dynamics (CFD) geometry (see figure). It automatically uses bicubic B-splines to extrapolate (if necessary) each surface in a conceptual geometry so that all the independently defined geometric components (such as wing and fuselage) can be intersected to form a watertight CFD geometry. The software also computes the intersection curves of surface patches at any resolution (up to 10^{-4} accuracy) specified by

the user, and it writes the B-spline surface patches, and the corresponding boundary points, for the watertight CFD geometry in the format that can be directly used by the grid generation tool VGRID.

iPatch requires that input geometry be in PLOT3D format where each component surface is defined by a rectangular grid $\{(x(i,j), y(i,j), z(i,j)): 1 \leq i \leq m, 1 \leq j \leq n\}$ that represents a smooth B-spline surface. All surfaces in the PLOT3D file conceptually represent a watertight geometry of components of an aircraft

on the half-space $y \geq 0$. Overlapping surfaces are not allowed, but could be fixed by a utility code "fixp3d". The fixp3d utility code first finds the two grid lines on the two surface grids that are closest to each other in Hausdorff distance (a metric to measure the discrepancies of two sets); then uses one of the grid lines as the transition line, extending grid lines on one grid to the other grid to form a merged grid.

Any two connecting surfaces shall have a "visually" common boundary curve, or can be described by an inter-



The iPatch Computer Code converts conceptual geometry (left) to corresponding CFD geometry (right).

section relationship defined in a geometry specification file. The intersection of two surfaces can be at a “conceptual” level. However, the intersection is direc-

tional (along either *i* or *j* index direction), and each intersecting grid line (or its spine extrapolation) on the first surface should intersect the second surface.

No two intersection relationships will result in a common intersection point of three surfaces.

The output files of iPatch are IGES, d3m, and mapbc files that define the CFD geometry in VGRID format. The IGES file gives the NURBS definition of the outer mold line in the geometry. The d3m file defines how the outer mold line is broken into surface patches whose boundary curves are defined by points. The mapbc file specifies what the boundary condition is on each patch and the corresponding NURBS surface definition of each non-planar patch in the IGES file.

This work was done by Wu Li of Langley Research Center. Further information is contained in a TSP (see page 1). LAR-17685-1

➤ Stereo Imaging Tactical Helper

NASA's Jet Propulsion Laboratory, Pasadena, California

The Stereo Imaging Tactical Helper (SITH) program displays left and right images in stereo using the display technology made available by the JADIS framework, which was described in “JAVA Stereo Display Toolkit,” *NASA Tech Briefs*, Vol. 32, No. 4 (April 2008), page 63. An overlay of the surface described by the disparity map (generated from the left and right images) allows the map to be compared to the actual images. In addition, an interactive cursor, whose visual depth is controlled by the disparity map, is used to ensure the correlated surface matches the real surface. This enhances the ability of operations personnel to provide quality control for correlation results, as well as to greatly assist developers working on correlation improvements. While its primary purpose is as a quality control tool

for inspecting correlation results, SITH is also straightforward for use as a basic stereo image viewer.

There are two modes for the image display: stereo (left/right) through hardware or anaglyph, and adjacent, where the right image pane is placed to the right or bottom of the left image pane. The mode is switchable at runtime. The application displays with left and right images with an overlaid cursor per image. The positions of the image pane cursors will be related such that, given the coordinates of the cursor center on the left image, the position of the right pane cursor will be the mapped coordinates found in the disparity file. In stereo mode, this constitutes a stereo cursor.

In grid mapping, a flat grid is painted over the left image, and on the right,

points from the left grid are mapped to the corresponding point on the right grid. This usually results in warping that indicates a higher-level view of the correlation result. As left and right images may not be adequately aligned such that they can be viewed comfortably, manual disparity controls exist to allow the right image to be shifted along the horizontal and vertical axes to produce stereo results that are easier for the user to view.

This work was done by Nicholas T. Toole of Caltech for NASA's Jet Propulsion Laboratory. For more information, contact iaoffice@jpl.nasa.gov.

This software is available for commercial licensing. Please contact Daniel Broderick of the California Institute of Technology at danielb@caltech.edu. Refer to NPO-46669.

➤ Planning and Execution for an Autonomous Aerobot

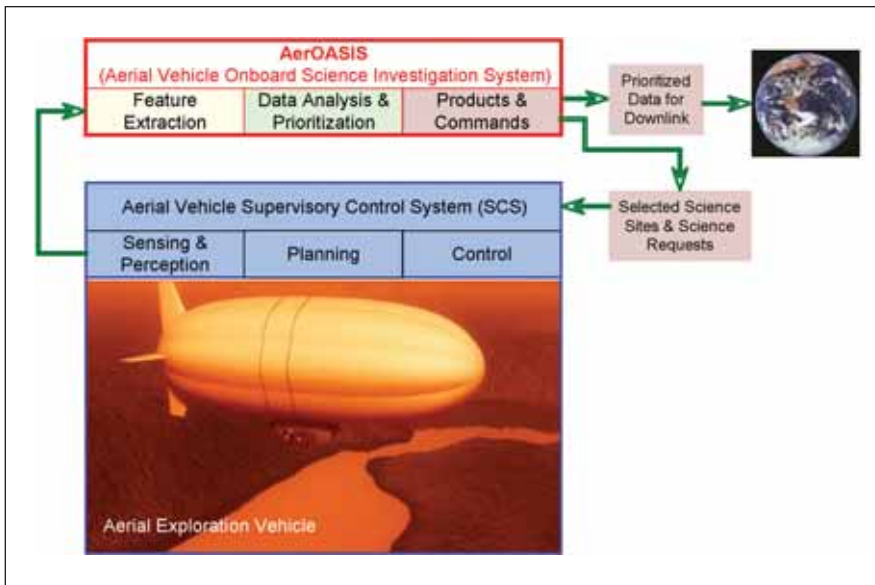
NASA's Jet Propulsion Laboratory, Pasadena, California

The Aerial Onboard Autonomous Science Investigation System (AerOASIS) system provides autonomous planning and execution capabilities for aerial vehicles (see figure). The system is capable of generating high-quality operations plans that integrate observation requests

from ground planning teams, as well as opportunistic science events detected onboard the vehicle while respecting mission and resource constraints.

AerOASIS allows an airborne planetary exploration vehicle to summarize and prioritize the most scientifically rel-

evant data; identify and select high-value science sites for additional investigation; and dynamically plan, schedule, and monitor the various science activities being performed, even during extended communications blackout periods with Earth.



The AerOASIS provides a number of functions in airborne planetary exploration.

AerOASIS system is composed of three main subsystems: Feature Extraction, which processes sensor im-

agery and other types of data (such as atmospheric pressure, temperature, wind speeds, etc.) and performs data

segmentation and feature extraction; Data Analysis and Prioritization, which matches the extracted feature vectors against scientist-defined signatures. The results are used to detect novelty, perform science data prioritization, and summarization for downlink, and identify and select high-value science sites for *in-situ* studies; and Planning and Scheduling, which generates operations plans to achieve observation requests submitted from Earth and from onboard data analysis. These science requests can include low-altitude, high-resolution surveys, *in-situ* sonde deployment, and/or surface sample acquisition for onboard analysis.

This work was done by Daniel M. Gaines, Tara A. Estlin, Steven R. Schaffer, and Caroline M. Chouinard of Caltech for NASA's Jet Propulsion Laboratory. For more information, contact iaoffice@jpl.nasa.gov.

This software is available for commercial licensing. Please contact Daniel Broderick of the California Institute of Technology at danielb@caltech.edu. Refer to NPO-46895.

➤ Real-Time Exponential Curve Fits Using Discrete Calculus

Novel curve fitting solution removes the limits, is robust, and is faster.

John F. Kennedy Space Center, Florida

An improved solution for curve fitting data to an exponential equation ($y = Ae^{Bt} + C$) has been developed. This improvement is in four areas — speed, stability, determinant processing time, and the removal of limits. The solution presented avoids iterative techniques and their stability errors by using three mathematical ideas: discrete calculus, a special relationship (between exponential curves and the Mean Value Theorem for Derivatives), and a simple linear curve fit algorithm. This method can also be applied to fitting data to the general power law equation

$y = Ax^B + C$ and the general geometric growth equation $y = Ak^{Bt} + C$.

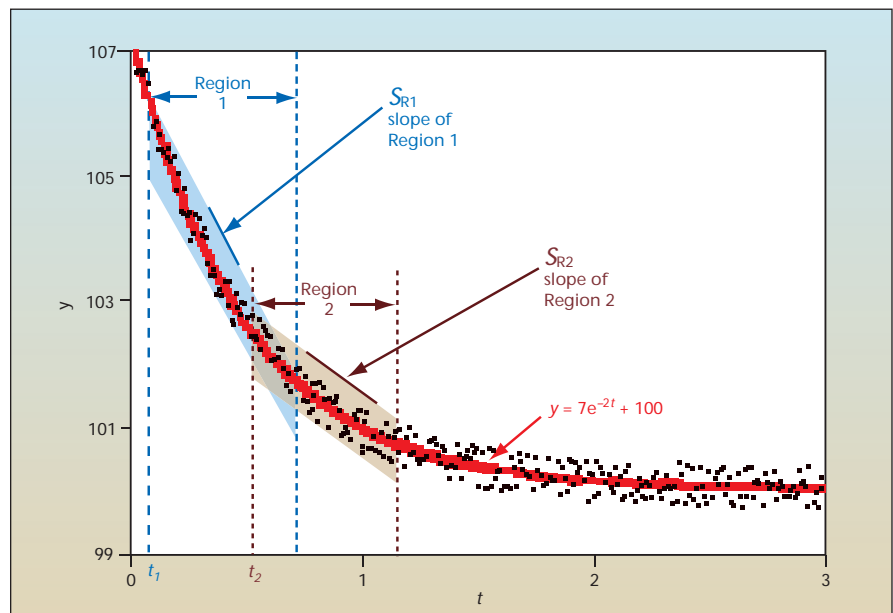
This improved method offers several advantages over prior exponential-curve-fitting methods. The advantages are as follows:

- Speed: Iterative (non-linear) methods are 50 to 100 times slower. Previously, only iterative methods could be used when C was not zero, or when all the samples were not zero or greater.
- Stability: No bad guesses. There is no chance of making a bad first guess as sometimes happens in iterative (non-

linear) techniques. Sometimes the iterative techniques “blow up” when they start with a bad guess.

- Real-Time requires determinism: Being faster would allow this method

to be used in real-time applications where non-linear methods take too much processing time. But, most real-time applications require determinism (a consistent processing time from



Two Regions of Points that overlap are shown. The slope ratios of these two regions are used in estimating B . In this example, $A = 7$, $B = -2$, and $C = 100$.

curve fit to curve fit, or at least a known maximum processing time). Iterative techniques vary greatly in the processing time they consume. This new method takes the same amount of processing time (for the same number of data points), no matter what the error distribution is. Iterative techniques sometimes only take 50 times longer and sometimes more than 100 times longer, depending on how the data varies and the initial guesses.

- y can cross zero: Even if $C = 0$, the non-iterative methods require all sample points to be zero or greater (or transformed to greater than zero). This method does not have any such limitation.

The improved method has a theoretical basis in discrete calculus, statistics, and regular calculus. The following description of the method omits most of the details of the theory for the sake of brevity.

The method is embodied in an algorithm for computing B in the equation $y = Ae^{Bt} + C$. Once B is known, typical linear methods can be used to solve for A and C . This method presents many ways to compute B . One way is by doing a linear (straight line) curve fit to two different regions in the data. The change in slope of these two regions gives us an estimate for B . The two different regions can even overlap each other to improve the curve fit. B is only

dependent on the change in slope and the change in time.

Let S_{R1} be the slope calculated for Region 1 (see figure). Let S_{R2} be the slope calculated for Region 2. Then the change in slope can be estimated by S_{R1}/S_{R2} . The time used to cause this change in slope is equal to the time between the first samples in each region (if each region contains the same number of equally spaced points). It can be shown that:

$$B = \ln(S_{R1}/S_{R2}) / (t_1 - t_2).$$

This work was done by Geoffrey Rowe of ASRC Aerospace Corp. for Kennedy Space Center. Further information is contained in a TSP (see page 1). KSC-13153

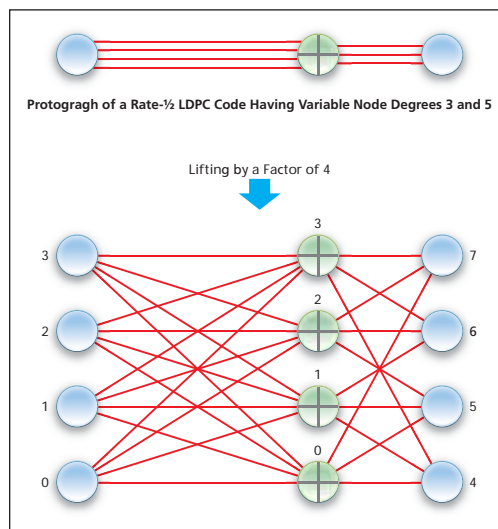
Short-Block Protograph-Based LDPC Codes

Characteristics of these codes include low undetected-error rates and low latency.

NASA's Jet Propulsion Laboratory, Pasadena, California

Short-block low-density parity-check (LDPC) codes of a special type are intended to be especially well suited for potential applications that include transmission of command and control data, cellular telephony, data communications in wireless local area networks, and satellite data communications. [In general, LDPC codes belong to a class of error-correcting codes suitable for use in a variety of wireless data-communication systems that include noisy channels.] The codes of the present special type exhibit low error floors, low bit and frame error rates, and low latency (in comparison with related prior codes). These codes also achieve low maximum rate of undetected errors over all signal-to-noise ratios, without requiring the use of cyclic redundancy checks, which would significantly increase the overhead for short blocks. These codes have protograph representations; this is advantageous in that, for reasons that exceed the scope of this article, the applicability of protograph representations makes it possible to design high-speed iterative decoders that utilize belief-propagation algorithms.

The codes of the present special type are characterized mainly by rate 1/2 and input block sizes of 64, 128, and 256 bits. To simplify encoder and decoder implementations for high-data-rate transmission, the structures of the codes are based on protographs (see figure) and



Construction of a Code of the present special type includes elaboration of a starting protograph in a process denoted in the art as "lifting." In this example, a starting protograph is first lifted by a factor of 4. In a subsequent step (not shown in the figure), the lifted-by-4 protograph is further lifted by a factor of 16 using circulant permutations.

circulants. These codes are designed for short blocks, the block sizes being based on maximizing minimum distances and stopping-set sizes subject to a constraint on the maximum variable node degree. In particular, these codes are designed to have variable node degrees between 3 and 5.

Short-block codes are desirable in communication systems in which frame-length constraints are imposed on the physical layers. For reasons that, once

again, exceed the scope of this article, avoidance of degree-2 nodes enables construction of codes having minimum distance that grows linearly with block size. Limiting code design to the use of variable node degrees ≥ 3 is sufficient, but not necessary, for minimum distance to grow linearly with block size. Increasing the node degree leads to larger minimum distance, at the expense of smaller girth. Therefore, there is an engineering compromise between undetected-error-rate performance (which is improved by increasing minimum distance) and the degree of suboptimality of iterative decoders typically used (which is adversely affected by graph loops).

Codes of the present special type were found to perform well in computational simulations. For example, for a code of input block size of 64, constructed from the protograph in the figure with variable node degrees 3 and 5, the maximum undetected-error rate was found to be $< 3 \times 10^{-5}$. This maximum was found to occur at a bit signal-to-noise ratio (SNR) of about 1.5, and the undetected-error rate was found to be smaller at SNRs both above and below 1.5, notably decreasing sharply with increasing SNR above 1.5.

This work was done by Dariush Divsalar, Samuel Dolinar, and Christopher Jones of Caltech for NASA's Jet Propulsion Laboratory. For more information, contact iaoffice@jpl.nasa.gov. NPO-45190

Space Images for NASA/JPL

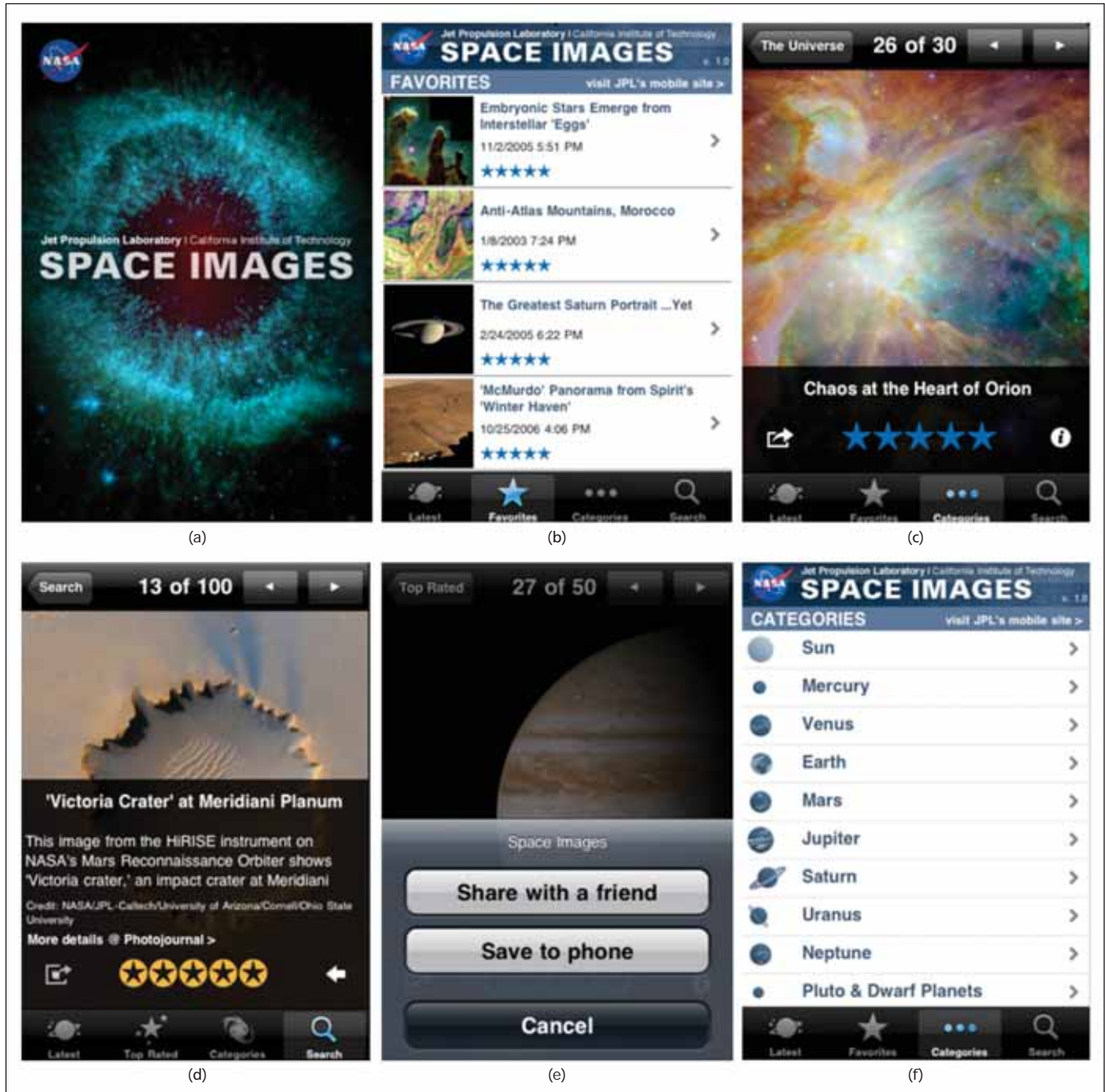
NASA's Jet Propulsion Laboratory, Pasadena, California

Space Images for NASA/JPL is an Apple iPhone application that allows the general public to access featured images from the Jet Propulsion Laboratory (JPL). A back-end infrastructure stores, tracks, and retrieves space images from the JPL Photojournal Web server, and catalogs the information into a streamlined rating infrastructure.

This system consists of four distinguishing components: image repository, database, server-side logic, and iPhone application. The image repository contains images from various JPL flight projects. The database stores the image information as well as the user rating. The server-side logic retrieves the image information from the database and cate-

gorizes each image for display. The iPhone application is an interfacing delivery system that retrieves the image information from the server for each Apple iPhone user. Also created is a reporting and tracking system for charting and monitoring usage.

Unlike other iPhone image applications, this system uses the latest



Here are a few Sample Screen Shots of the Space Images iPhone Application: The splash screen (a) is displayed during the initial application start up. The title and image thumbnails (b) are scrollable lists. When clicked, it will show the images in detail, as well as a caption describing the image (c), (d). The user can rate the images by giving a star rating from 1 to 5. In addition, there is an option to share the image by e-mail or save it to the user's iPhone (e). Images can also be retrieved through their categories or from the search results (f).

emerging technologies to produce image listings based directly on user input. This allows for countless combinations of images returned. The backend infrastructure uses industry-standard coding and database methods, enabling future software improvement and technology updates. The flexibility of the system design framework permits multiple levels of display pos-

sibilities and provides integration capabilities.

Unique features of the software include image retrieval from a selected set of categories, image Web links that can be shared among e-mail users, and image metadata searchable for instant results (see figure).

This work was done by Karen Boggs, Sandy C. Gutheinz, Susan M. Watanabe,

Boris Oks, Jeremy M. Arca, Alice Stanboli, Martin Perez, Rebecca Whatmore, Minliang Kang, and Luis A. Espinoza of Caltech and Justin Moore of Moore Boeck for NASA's Jet Propulsion Laboratory. For more information, contact iaoffice@jpl.nasa.gov.

This software is available for commercial licensing. Please contact Daniel Broderick of the California Institute of Technology at danielb@caltech.edu. Refer to NPO-47264.

➤ Situational Lightning Climatologies

This technique assists in the preparation of lightning forecasts for aviation, power companies, and sporting-event applications.

John F. Kennedy Space Center, Florida

Research has revealed distinct spatial and temporal distributions of lightning occurrence that are strongly influenced by large-scale atmospheric flow regimes. It was believed there were two flow systems, but it has been discovered that actually there are seven distinct flow regimes.

The Applied Meteorology Unit (AMU) has recalculated the lightning climatologies for the Shuttle Landing Facility (SLF), and the eight airfields in the National Weather Service in Melbourne (NWS MLB) County Warning Area (CWA) using individual lightning strike data to improve the accuracy of the climatologies. A 19-year record of cloud-to-ground (CG) lightning strikes was assembled and manipulated into a usable database of lightning information based on day and time of occurrence, distance from the airfield, and wind flow regime. The software determines the location of each CG lightning strike with 5-, 10-, 20-, and 30-nmi (≈9.3-, 18.5-, 37-, 55.6-km) radii from each airfield. Each CG lightning strike is binned at 1-, 3-, and 6-hour intervals at each specified radius. The software merges the CG lightning strike time intervals and distance with each wind flow regime and creates probability statistics for each time interval, radii, and flow regime, and stratifies them by month and warm season.

The AMU also updated the graphical user interface (GUI) with the new data. As in the previous phase, the AMU stratified the climatologies for each location by time interval, distance, and flow regime. New for this phase, the AMU included all data regardless of flow regime as one of the stratifications, added monthly stratifi-



This Map of Central Florida shows the locations of nine sites in the NWS MLB CWA surrounded by 5-, 10-, 20-, and 30-nmi (≈9.3-, 18.5-, 37-, 55.6-km) radius range rings. The Applied Meteorology Unit made changes such that the 5- and 10-nmi (≈9.3- and 18.5-km) radius range rings are consistent with the aviation forecast requirements at NSW MLB.

cations, used modified flow regimes, and added three years of data to the period of record.

The AMU used individual strike data from the National Lightning Detection Network (NLDN) instead of NLDN-gridded lightning data to create more accurate climatological values for each range ring than was possible with the gridded data set. Individual strike data is more advantageous than gridded strike data because it simplifies the data processing, it provides more accurate climatologies, and it does not require estimating circular range rings from square grids.

In addition, to better meet customer requirements, the AMU made changes such that the 5- and 10-nmi (≈9.3- and 18.5-km) radius range rings are consistent with the aviation forecast requirements at NWS MLB, while the 20- and 30-nmi (≈37- and 55.6-km) radius range rings at the SLF assist Spaceflight Metrology Group (SMG) in making forecasts for weather Flight Rule violations of lightning occurrence during a shuttle landing.

This work was done by William Bauman and Winifred Crawford of ENSCO, Inc. for Kennedy Space Center. Further information is contained in a TSP (see page 1). KSC-13374

Autonomous Exploration for Gathering Increased Science

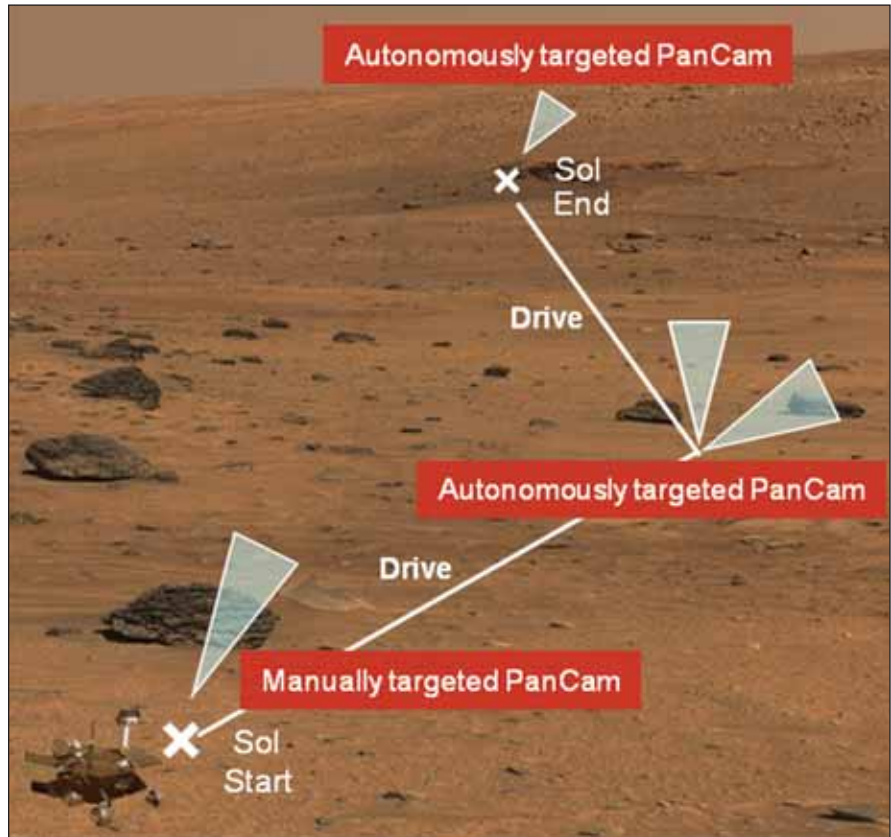
NASA's Jet Propulsion Laboratory, Pasadena, California

The Autonomous Exploration for Gathering Increased Science System (AEGIS) provides automated targeting for remote sensing instruments on the Mars Exploration Rover (MER) mission, which at the time of this reporting has had two rovers exploring the surface of Mars (see figure). Currently, targets for rover remote-sensing instruments must be selected manually based on imagery already on the ground with the operations team. AEGIS enables the rover flight software to analyze imagery onboard in order to autonomously select and sequence targeted remote-sensing observations in an opportunistic fashion. In particular, this technology will be used to automatically acquire sub-framed, high-resolution, targeted images taken with the MER panoramic cameras.

This software provides:

- Automatic detection of terrain features in rover camera images,
- Feature extraction for detected terrain targets,
- Prioritization of terrain targets based on a scientist target feature set, and
- Automated re-targeting of rover remote-sensing instruments at the highest priority target.

This work was done by Benjamin J. Bornstein, Rebecca Castano, Tara A. Estlin, Daniel M. Gaines, Robert C. Anderson, David R. Thompson, Charles K. De Granville, Steve A. Chien, Benyang Tang,



New MER Capability is shown for automated targeting.

Michael C. Burl, and Michele A. Judd of Caltech for NASA's Jet Propulsion Laboratory. For more information, contact iaoffice@jpl.nasa.gov.

This software is available for commercial licensing. Please contact Daniel Broderick of the California Institute of Technology at danielb@caltech.edu. Refer to NPO-46876.

World Wide Web Metaphors for Search Mission Data

NASA's Jet Propulsion Laboratory, Pasadena, California

A software program that searches and browses mission data emulates a Web browser, containing standard metaphors for Web browsing. By taking advantage of back-end URLs, users may save and share search states. Also, since a Web interface is familiar to users, training time is reduced. Familiar back and forward buttons move through a local search history. A refresh/reload button regenerates a query, and loads in any new data. URLs can be constructed to save search results.

Adding context to the current search is also handled through a familiar Web

metaphor. The query is constructed by clicking on hyperlinks that represent new components to the search query. The selection of a link appears to the user as a page change; the choice of links changes to represent the updated search and the results are filtered by the new criteria. Selecting a navigation link changes the current query and also the URL that is associated with it. The back button can be used to return to the previous search state. This software is part of the MSLICE release, which was written in Java. It will run on any current Windows, Macintosh, or Linux system.

This work was done by Jeffrey S. Norris, Michael N. Wallick, Joseph C. Joswig, Mark W. Powell, Recaredo J. Torres, David S. Mittman, Lucy Abramyan, Thomas M. Crockett, Khawaja S. Shams, and Jason M. Fox of Caltech and Melissa Ludowise of Ames Research Center for NASA's Jet Propulsion Laboratory. For more information, contact iaoffice@jpl.nasa.gov.

This software is available for commercial licensing. Please contact Daniel Broderick of the California Institute of Technology at danielb@caltech.edu. Refer to NPO-46832.

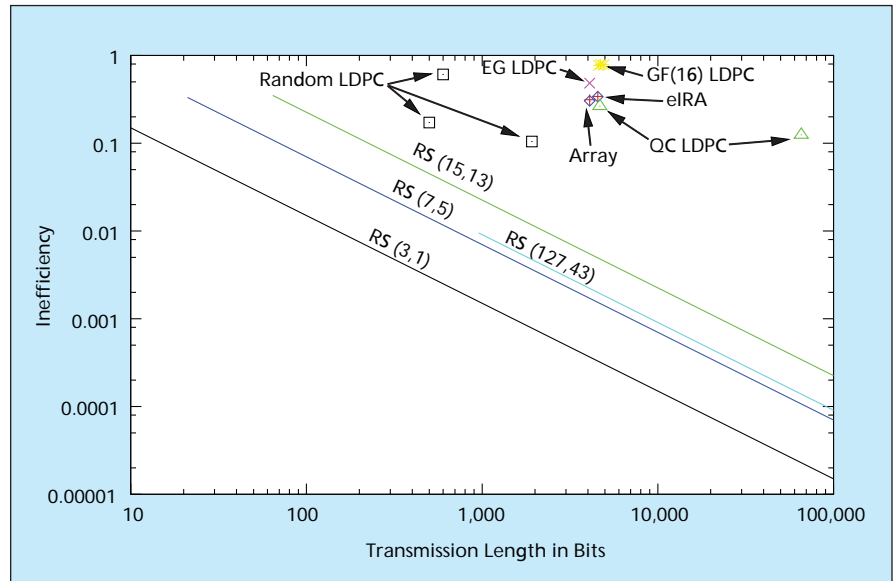
Optimal Codes for the Burst Erasure Channel

This approach offers lower decoding complexity with better burst erasure protection.

NASA's Jet Propulsion Laboratory, Pasadena, California

Deep space communications over noisy channels lead to certain packets that are not decodable. These packets leave gaps, or bursts of erasures, in the data stream. Burst erasure correcting codes overcome this problem. These are forward erasure correcting codes that allow one to recover the missing gaps of data. Much of the recent work on this topic concentrated on Low-Density Parity-Check (LDPC) codes. These are more complicated to encode and decode than Single Parity Check (SPC) codes or Reed-Solomon (RS) codes, and so far have not been able to achieve the theoretical limit for burst erasure protection.

A block interleaved maximum distance separable (MDS) code (e.g., an SPC or RS code) offers near-optimal burst erasure protection, in the sense that no other scheme of equal total transmission length and code rate could improve the guaranteed correctable burst erasure length by more than one symbol. The optimality does not depend on the length of the code, i.e., a short MDS code block interleaved to a given length would perform as well as a longer MDS code interleaved to the same overall length. As a result, this approach offers lower decoding complexity with better burst erasure protection compared to other recent designs for the burst erasure channel (e.g., LDPC codes). A limitation of the design is its lack of robustness to channels that have impairments



The Inefficiency of Interleaved RS Codes is compared with other listed codes.

other than burst erasures (e.g., additive white Gaussian noise), making its application best suited for correcting data erasures in layers above the physical layer. The efficiency of a burst erasure code is the length of its burst erasure correction capability divided by the theoretical upper limit on this length. The inefficiency is one minus the efficiency. The illustration compares the inefficiency of interleaved RS codes to Quasi-Cyclic (QC) LDPC codes, Euclidean Geometry (EG) LDPC codes, extended Irregular Repeat Accumulate (eIRA) codes, array

codes, and random LDPC codes previously proposed for burst erasure protection. As can be seen, the simple interleaved RS codes have substantially lower inefficiency over a wide range of transmission lengths.

This work was done by Jon Hamkins of Caltech for NASA's Jet Propulsion Laboratory. For more information, contact iaofflce@jpl.nasa.gov.

The software used in this innovation is available for commercial licensing. Please contact Daniel Broderick of the California Institute of Technology at danielb@caltech.edu. Refer to NPO-46903.

Phenological Parameters Estimation Tool

NASA's Jet Propulsion Laboratory, Pasadena, California

The Phenological Parameters Estimation Tool (PPET) is a set of algorithms implemented in MATLAB that estimates key vegetative phenological parameters. For a given year, the PPET software package takes in temporally processed vegetation index data (3D spatio-temporal arrays) generated by the time series product tool (TSPT) and outputs spatial grids (2D arrays) of vegetation phenological parameters. As a precursor to PPET, the TSPT uses quality information for each pixel of each date to remove bad or suspect data, and then interpo-

lates and digitally fills data voids in the time series to produce a continuous, smoothed vegetation index product. During processing, the TSPT displays NDVI (Normalized Difference Vegetation Index) time series plots and images from the temporally processed pixels. Both the TSPT and PPET currently use moderate resolution imaging spectroradiometer (MODIS) satellite multispectral data as a default, but each software package is modifiable and could be used with any high-temporal-rate remote sensing data collection system that is ca-

pable of producing vegetation indices.

Raw MODIS data from the Aqua and Terra satellites is processed using the TSPT to generate a filtered time series data product. The PPET then uses the TSPT output to generate phenological parameters for desired locations. PPET output data tiles are mosaicked into a Conterminous United States (CONUS) data layer using ERDAS IMAGINE, or equivalent software package. Mosaics of the vegetation phenology data products are then reprojected to the desired map projection using ERDAS IMAGINE.

The TSPT software can temporally process a variety of MODIS multispectral data products on a per-pixel basis. Generally, the TSPT runs on one user-specified kind of MODIS data product to generate a given time series data product. The TSPT can process output from the MODIS Re-projection Tool (MRT) as input, or can directly convert MODIS Hierarchical Data Format (HDF) sinusoidal gridded data to BSQ input files.

Unlike other known vegetation phenological parameter estimation software, the PPET produces not only common phenological parameters, but also real-time and custom parameters without *a priori* assumptions about the shape of the phenological cycle. Common phe-

nological parameters, like those produced in PPET, are associated with the annual vegetation growth cycle. They quantitatively describe vegetative states related to annual cyclical growing seasons, such as green-up, maturity, senescence, and dormancy by analyzing the temporal shape of given vegetation index time series. The real-time phenological and custom parameters are formed from a cumulative sum (integral) produced at a fixed temporal interval. In addition, cumulative vegetation index and time-specific/pest-specific phenological parameters can be designed to optimize the detection of vegetation damage from specific pests and diseases. These problem-specific, phenological parameters have the potential to

be integrated into near real-time, predictive surveillance systems (i.e. early warning systems) and, with improved vegetative state information, could assist decision makers in making intelligent vegetation and associated land resource management choices.

This work was done by Rodney D. McKelip of Stennis Space Center; Kenton W. Ross, Joseph P. Spruce, James C. Smoot, and Robert E. Ryan of Science Systems and Applications, Inc.; Gerald E. Gasser of Lockheed Martin; and Donald L. Prados and Ronald D. Vaughan of Computer Sciences Corp.

Inquiries concerning rights for the commercial use of this invention should be addressed to the Intellectual Property Manager at Stennis Space Center (228) 688-1929. SSC-00321

XMbodyinfo

NASA's Jet Propulsion Laboratory, Pasadena, California

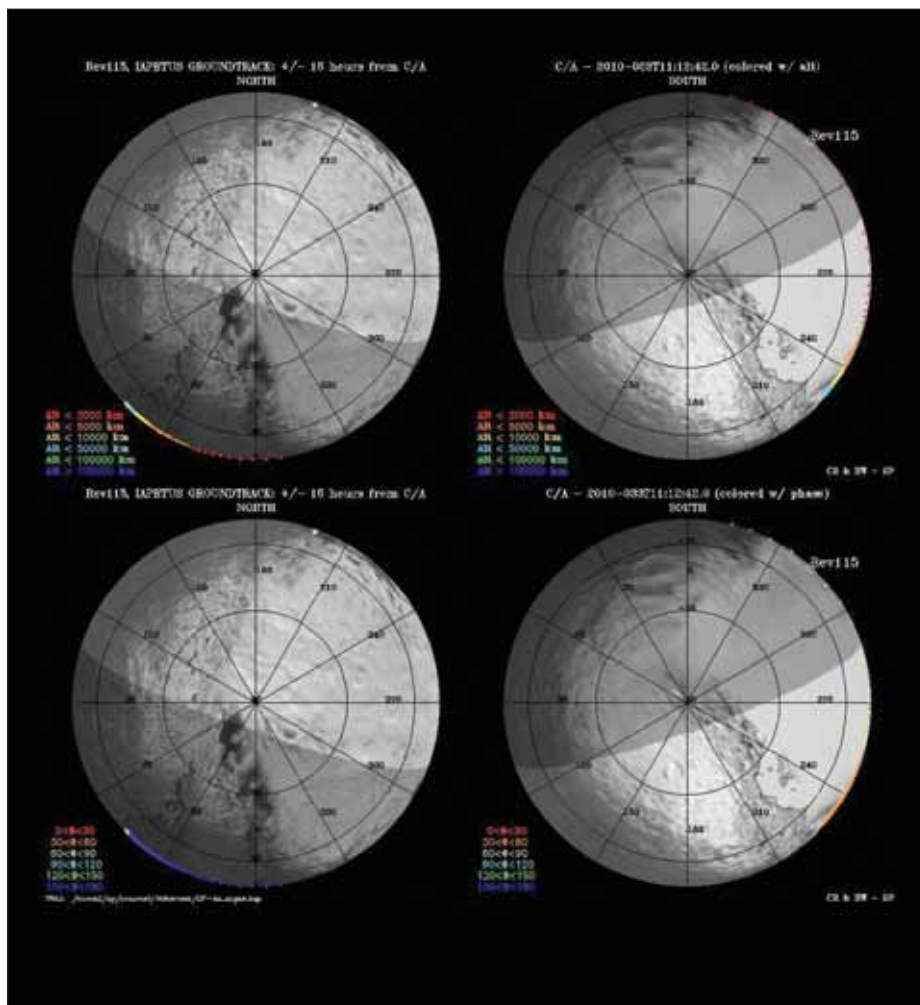
XMbodyinfo was designed to evaluate potential reference trajectories, providing a proficient way to assess the quality of all satellite body flybys for a Cassini type mission tour. It is autonomous and will generate a variety of ORS (optical remote sensing) and FPW (fields, particles, and waves) plots that aid in the evaluation, qualification, selection, and improvement of a potential tour (see figure).

XMbodyinfo attempts to streamline the tour design process. More specifically, it attempts to streamline the approval process, interaction, and subsequent iteration that must occur between the tour designers and the science teams during the design and development of a tour.

It can quickly produce various geometry plots and ground tracks for Saturnian satellite flybys when given an input trajectory, a C/A (closest approach) time in SCET (Spacecraft Event Time), and a flyby label. All instrument teams and science disciplines used this tool extensively to aid in the selection of Cassini's extended mission tour.

This work was done by Chris Roumeliotis and Bradford D. Wallis of Caltech for NASA's Jet Propulsion Laboratory. For more information, contact iaoffice@jpl.nasa.gov.

This software is available for commercial licensing. Please contact Daniel Broderick of the California Institute of Technology at danielb@caltech.edu. Refer to NPO-46482.



Individual Flyby Groundtrack Plot is color coded with altitude and phase angle (polar projection). This is one of a number of plots provided by XMbodyinfo.

➤ Centralized Alert-Processing and Asset Planning for Sensorwebs

NASA's Jet Propulsion Laboratory, Pasadena, California

A software program provides a Sensorweb architecture for alert-processing, event detection, asset allocation and planning, and visualization (see figure). It automatically tasks and re-tasks various types of assets such as satellites and robotic vehicles in response to alerts (fire, weather) extracted from various data sources, including low-level Webcam data. JPL has adapted considerable Sensorweb infrastructure that had been previously applied to

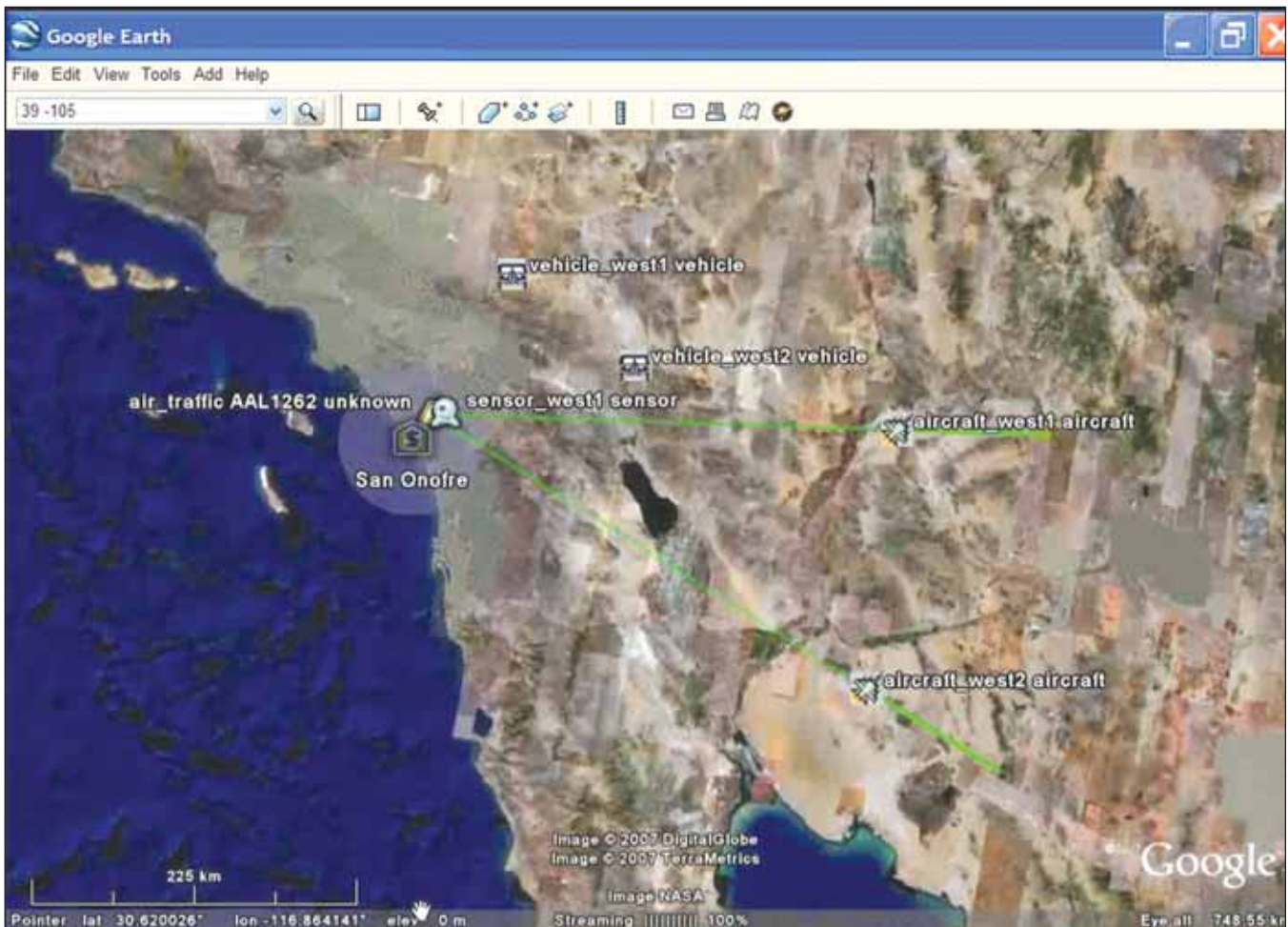
NASA Earth Science applications. This NASA Earth Science Sensorweb has been in operational use since 2003, and has proven reliability of the Sensorweb technologies for robust event detection and autonomous response using space and ground assets.

Unique features of the software include flexibility to a range of detection and tasking methods including those that require aggregation of data over spatial and temporal ranges, generality of the re-

sponse structure to represent and implement a range of response campaigns, and the ability to respond rapidly.

This work was done by Rebecca Castano, Steve A. Chien, Gregg R. Rabideau, and Benyang Tang of Caltech for NASA's Jet Propulsion Laboratory. For more information, contact iaoffice@jpl.nasa.gov.

This software is available for commercial licensing. Please contact Daniel Broderick of the California Institute of Technology at danielb@caltech.edu. Refer to NPO-46468.



The Map is updated to show both planned asset routes as well as actual routes taken.

➤ Support for Systematic Code Reviews With the SCRUB Tool

NASA's Jet Propulsion Laboratory, Pasadena, California

SCRUB is a code review tool that supports both large, team-based software development efforts (e.g., for mission software) as well as individual tasks. The tool was developed at JPL to support a new,

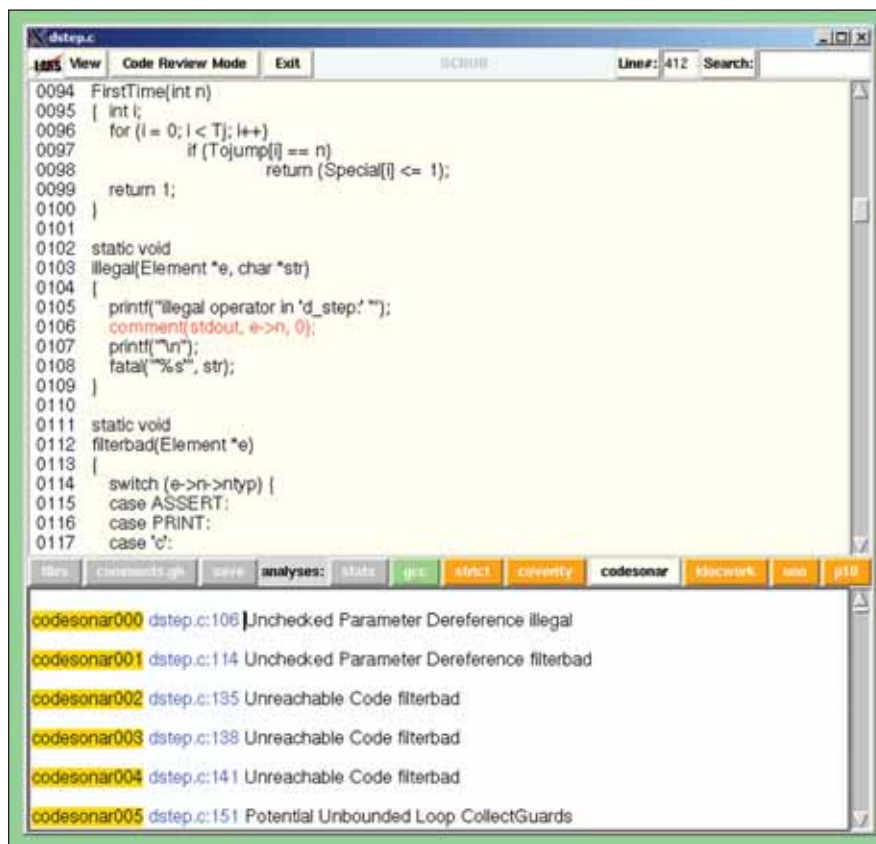
streamlined code review process that combines human-generated review reports with program-generated review reports from a customizable range of state-of-the-art source code analyzers. The

leading commercial tools include Codeonar, Coverity, and Klocwork, each of which can achieve a reasonably low rate of false-positives in the warnings that they generate. The time required to analyze

code with these tools can vary greatly. In each case, however, the tools produce results that would be difficult to realize with human code inspections alone. There is little overlap in the results produced by the different analyzers, and each analyzer used generally increases the effectiveness of the overall effort. The SCRUB tool allows all reports to be accessed through a single, uniform interface (see figure) that facilitates browsing code and reports. Improvements over existing software include significant simplification, and leveraging of a range of commercial, static source code analyzers in a single, uniform framework.

The tool runs as a small stand-alone application, avoiding the security problems related to tools based on Web-browsers. A developer or reviewer, for instance, must have already obtained access rights to a code base before that code can be browsed and reviewed with the SCRUB tool. The tool cannot open any files or folders to which the user does not already have access. This means that the tool does not need to enforce or administer any additional security policies. The analysis results presented through the SCRUB tool's user interface are always computed off-line, given that, especially for larger projects, this computation can take longer than appropriate for interactive tool use.

The recommended code review process that is supported by the SCRUB tool consists of three phases: Code Review, Developer Response, and Closeout Resolution. In the Code Review phase, all tool-based analysis reports are generated, and specific comments from expert code reviewers are entered into the SCRUB



SCRUB User Interface is shown when it is opened in local mode.

tool. In the second phase, Developer Response, the developer is asked to respond to each comment and tool-report that was produced, either agreeing or disagreeing to provide a fix that addresses the issue that was raised. In the third phase, Closeout Resolution, all disagreements are discussed in a meeting of all parties involved, and a resolution is made for all disagreements. The first two phases generally take

one week each, and the third phase is concluded in a single closeout meeting.

This work was done by Gerard J. Holzmann of Caltech for NASA's Jet Propulsion Laboratory. Further information is contained in a TSP (see page 1).

This software is available for commercial licensing. Please contact Daniel Broderick of the California Institute of Technology at danielb@caltech.edu. Refer to NPO-46817.

Numerical Mean Element Orbital Analysis With Morbiter

NASA's Jet Propulsion Laboratory, Pasadena, California

The Morbiter software numerically averages an osculating orbit's equations of motion (EOM) to arrive at the mean orbit's EOMs, which are then numerically propagated to obtain the long-term orbital ephemerides. The long-term evolution characteristics, and stability, of an orbit are best characterized using a mean element propagation of the perturbed, two-body variational equations of motion. The average process eliminates short period terms, leaving only secular and long period effects. Doing this avoids the Fourier series expansions and truncations required by the traditional analytic methods.

The numerical methods require no analytic approximation, and the averaging theory and software implementation work at any solar system body. JPL's Monte mission analysis and navigation software was used as the underlying trajectory system (to the extent possible) for this innovation.

Morbiter is a package of Python scripts that implement the algorithms, and uses Monte for basic astrodynamics constructs and functions such as trajectories, ephemerides, coordinate systems, astrodynamics constants, and, in most cases, the perturbation acceleration methods. Python is an interpreted language that

provides an ideal platform for rapid development of algorithms; however, there is a performance penalty for using Python script-based applications. An end-user, future version of Morbiter that is fully compiled will not suffer from this speed penalty; development of this version is planned to begin in late FY '10.

This work was done by Todd A. Ely of Caltech for NASA's Jet Propulsion Laboratory. For more information, contact iaoffice@jpl.nasa.gov.

This software is available for commercial licensing. Please contact Daniel Broderick of the California Institute of Technology at danielb@caltech.edu. Refer to NPO-47212.

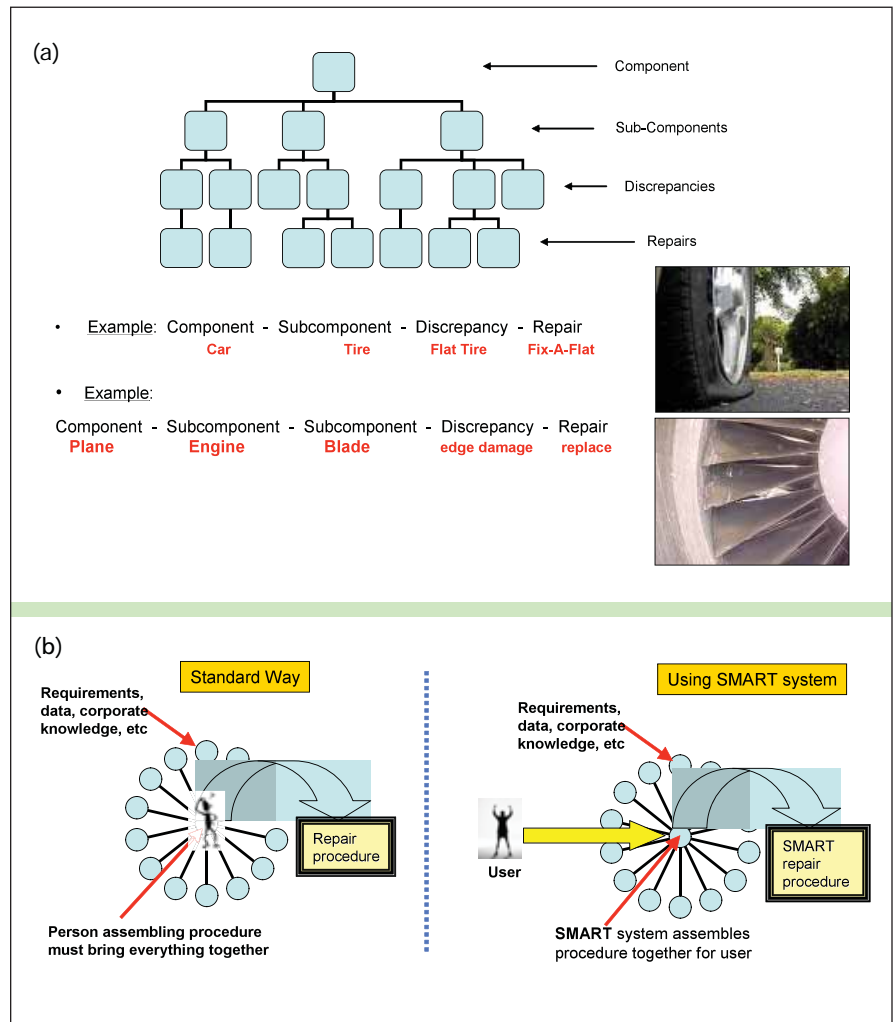
Systems Maintenance Automated Repair Tasks (SMART)

John F. Kennedy Space Center, Florida

SMART is a uniform automated discrepancy analysis and repair-authoring platform that improves technical accuracy and timely delivery of repair procedures for a given discrepancy (see figure a). SMART will minimize data errors, create uniform repair processes, and enhance the existing knowledge base of engineering repair processes. This innovation is the first tool developed that links the hardware specification requirements with the actual repair methods, sequences, and required equipment. SMART is flexibly designed to be useable by multiple engineering groups requiring decision analysis, and by any work authorization and disposition platform (see figure b).

The organizational logic creates the link between specification requirements of the hardware, and specific procedures required to repair discrepancies. The first segment in the SMART process uses a decision analysis tree to define all the permutations between component/subcomponent/discrepancy/repair on the hardware. The second segment uses a repair matrix to define what the steps and sequences are for any repair defined in the decision tree. This segment also allows for the selection of specific steps from multivariable steps.

SMART will also be able to interface with outside databases and to store information from them to be inserted into the repair-procedure document. Some of the steps will be identified as optional, and would only be used based on the location and the current configuration of the hardware. The output from this analysis would be sent to a work authoring system in the form of a predefined sequence of steps containing required actions, tools, parts, materials, certifications, and spe-



SMART Solution to Problems: (a) simplistic example; (b) solution philosophy — variables.

cific requirements controlling quality, functional requirements, and limitations.

This work was done by Joseph Schuh of Kennedy Space Center and Brent Mitchell, Louis Locklear, Martin A. Belson, Mary Jo Y.

Al-Shihabi, Nadean King, Elkin Norena, and Derek Hardin of USA Spaceops. For more information, contact the Kennedy Innovative Partnerships Program Office at (321) 867-5033. KSC-12909

NAIF Toolkit — Extended

NASA's Jet Propulsion Laboratory, Pasadena, California

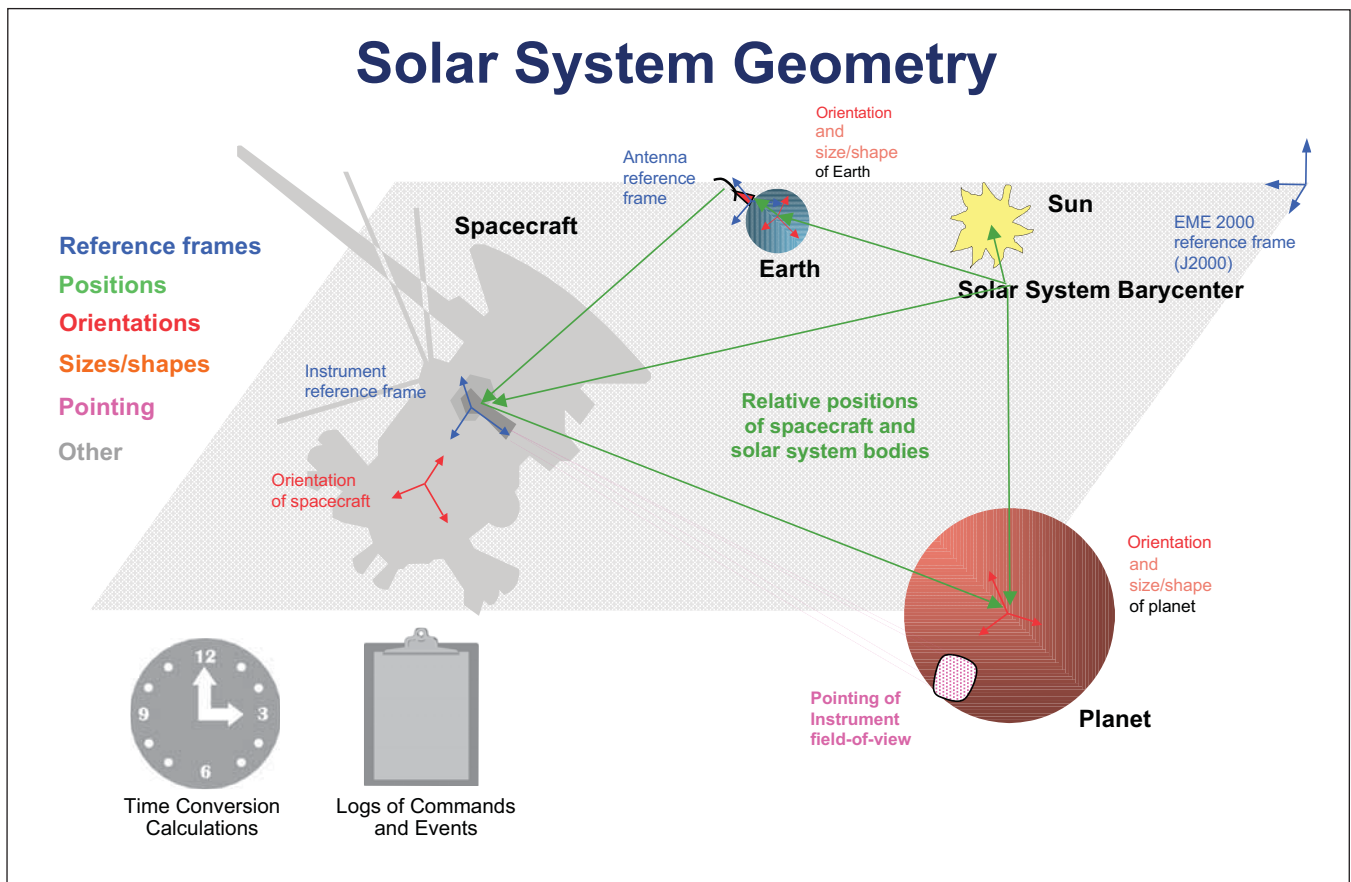
The Navigation Ancillary Information Facility (NAIF) at JPL, acting under the direction of NASA's Office of Space Science, has built a data system named SPICE (Spacecraft Planet Instrument C-matrix Events) to assist scientists in planning and interpreting scientific observations (see figure). SPICE provides

geometric and some other ancillary information needed to recover the full value of science instrument data, including correlation of individual instrument data sets with data from other instruments on the same or other spacecraft.

This data system is used to produce space mission observation geometry

data sets known as SPICE kernels. It is also used to read SPICE kernels and to compute derived quantities such as positions, orientations, lighting angles, etc. The SPICE toolkit consists of a subroutine/function library, executable programs (both large applications and simple utilities that focus on kernel

Solar System Geometry



An Overview of SPICE.

management), and simple examples of using SPICE toolkit subroutines.

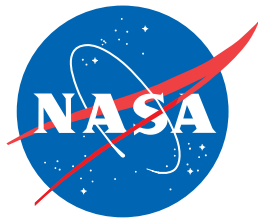
This software is very accurate, thoroughly tested, and portable to all computers. It is extremely stable and reusable on all missions. Since the previous version, three significant capabilities

have been added: Interactive Data Language (IDL) interface, MATLAB interface, and a geometric event finder subsystem.

This work was done by Charles H. Acton, Jr., Nathaniel J. Bachman, Boris V. Semenov, and Edward D. Wright of Caltech for NASA's

Jet Propulsion Laboratory. For more information, see <http://naif.jpl.nasa.gov>.

The software used in this innovation is available for commercial licensing. Please contact Daniel Broderick of the California Institute of Technology at danielb@caltech.edu. Refer to NPO-47017.



National Aeronautics and
Space Administration